

Scale dependency of regional climate modeling of current and future climate extremes in Germany

Merja H. Tölle¹  · Lukas Schefczyk² · Oliver Gutjahr³

Received: 22 March 2017 / Accepted: 12 October 2017 / Published online: 4 November 2017
© The Author(s) 2017. This article is an open access publication

Abstract A warmer climate is projected for mid-Europe, with less precipitation in summer, but with intensified extremes of precipitation and near-surface temperature. However, the extent and magnitude of such changes are associated with creditable uncertainty because of the limitations of model resolution and parameterizations. Here, we present the results of convection-permitting regional climate model simulations for Germany integrated with the COSMO-CLM using a horizontal grid spacing of 1.3 km, and additional 4.5- and 7-km simulations with convection parameterized. Of particular interest is how the temperature and precipitation fields and their extremes depend on the horizontal resolution for current and future climate conditions. The spatial variability of precipitation increases with resolution because of more realistic orography and physical parameterizations, but values are overestimated in summer and over mountain ridges in all simulations compared to observations. The spatial variability of temperature is improved at a resolution of 1.3 km, but the results are cold-biased, especially in summer. The increase in resolution from 7/4.5 km to 1.3 km is accompanied by less future warming in summer by 1 °C. Modeled future

precipitation extremes will be more severe, and temperature extremes will not exclusively increase with higher resolution. Although the differences between the resolutions considered (7/4.5 km and 1.3 km) are small, we find that the differences in the changes in extremes are large. High-resolution simulations require further studies, with effective parameterizations and tunings for different topographic regions. Impact models and assessment studies may benefit from such high-resolution model results, but should account for the impact of model resolution on model processes and climate change.

Keywords Climate change · Temperature extremes · Precipitation extremes · Regional climate model · Convection-permitting · Dynamical downscaling

1 Introduction

Global atmospheric CO₂ concentration will increase in the future because of anthropogenic emissions and cause relatively rapid climate change (Christensen et al. 2007; IPCC 2014). This climate change will affect the mean state of the climate and, in particular, its extreme events (IPCC 2007). Any changes in the frequency or intensity of extremes may impact nature and human society. Therefore, decision-makers in the public and private sectors require local-scale projections and detailed information to develop suitable adaptation strategies.

The temperate region Germany in the mid-latitudes, with its diverse landscapes and topography, serves as an ideal example of where finer-resolution climatology is needed. This region is influenced by a maritime climate in the north and by a continental climate in the south. General circulation models (GCMs) are inadequate to represent the

✉ Merja H. Tölle
Merja.Toelle@geogr.uni-giessen.de

¹ Department of Geography, Climatology, Climate Dynamics and Climate Change, Justus-Liebig-University Giessen, Senckenbergstr. 1, 35390 Giessen, Germany

² Department of Environmental Meteorology, University of Trier, Trier, Germany

³ Max Planck Institute for Meteorology, Hamburg, Germany

local climate variability associated with heterogeneous land cover, mountain chains (Zubler et al. 2015), and diverse coastlines. A regional climate model (RCM) is integrated only over a specific area, but with a much finer resolution than the forcing GCM (Dee et al. 2011). It is assumed that higher-resolution simulations lead to an improved representation of the physical processes in the models (Berg et al. 2013), where local features (such as topography and coastal processes) affect atmospheric flow (Kotlarski et al. 2014). Tselioudis et al. (2012) noted that higher-resolution models produced precipitation amounts that did not occur in the driving model. Maraun et al. (2010) showed that the ability of RCMs to simulate the spatial and temporal characteristics of rainfall increases with higher model resolution. Moreover, a denser grid spacing is expected to improve, for example, the representation of mesoscale circulation and the distribution of the intensity of daily precipitation (Ban et al. 2014).

Research efforts regarding spatial scales in climate downscaling are ongoing. The typical resolution applied for RCMs in the European project PRUDENCE (Christensen and Christensen 2007) was 50 km. A warm bias relative to observations in extreme seasons and a tendency toward a cold bias in transition seasons were reported (Jacob et al. 2007). The next collaborative effort, ENSEMBLES (Hewitt 2004; van der Linden and Mitchell 2009), applied spatial resolutions of 25 km. Although high-resolution models improve the accuracy of spatio-temporal precipitation characteristics, all ENSEMBLES RCMs exhibit a wet bias of about 20% in winter and about 10% in summer (Rauscher et al. 2010). In the downscaling experiments with COSMO-CLM (CCLM, COnsortium for Small-scale MOdeling-Climate Limited-area Model; Rockel et al. 2008), named consortial runs, resolution increased further down to 18 km (Hollweg et al. 2008). The recent Coordinated Regional Downscaling Experiment (CORDEX; Giorgi et al. 2009) addresses the improvements and climate change signals in the RCM climate simulations. Giorgi et al. (2016) demonstrated that dynamical downscaling to 12.5 km horizontal grid spacings over Europe introduces changes in climate that were not present in the forcing model. Kotlarski et al. (2014) found that the ERA-Interim driven EURO-CORDEX (the European branch of CORDEX) ensemble simulations largely confirm RCM bias characteristics identified from the previous ENSEMBLES data. The results show future increases in climate extremes, such as heat waves, droughts, and heavy rainfall (Vautard et al. 2013).

However, at such resolutions, deep convection is parameterized and leads to an overestimation of the net heat transport, rainfall rates, and the net strength of deep convection systems (Prein et al. 2013). As a result, such resolutions are still too coarse to capture climate variability at sub-grid scales. In addition, the number of investigations of local extremes remain limited, and such estimates, therefore,

still have high uncertainty. The more intense and frequent precipitation extremes enhance flooding potential (Trenberth et al. 2003). Enhanced flooding is expected to cause severe socio-economic damage and is thus of primary concern. Dynamical downscaling to higher horizontal resolution down to 1 km may overcome many of the problems of unresolved scales.

The emerging convection-permitting simulations (e.g., Kendon et al. 2014; Tölle et al. 2014; Ban et al. 2015; Gutjahr et al. 2016) show significant differences between high- and low-resolution models. Kilometer-scale models are termed convection-permitting because they begin to represent deep convection explicitly, whereas smaller plumes and showers are not resolved, with shallow convection left parameterized. Several authors (e.g., Hohenegger et al. 2009; Froidevaux et al. 2014) have shown that soil moisture-precipitation feedback reverses in sign at the convection-permitting scale, but with moderating effects on the hydrological cycle. Results with convection-permitting simulations indicate improved spatio-temporal characteristics of heavy hourly events (Ban et al. 2014; Chan et al. 2014b), and a better scaling with temperature (Ban et al. 2014). Further, the convection-permitting approach improves the simulation of the diurnal cycle of summer precipitation (Hohenegger et al. 2008; Prein et al. 2013). Tölle et al. (2014) demonstrated that the influence of land use/cover change is more pronounced when considering the convection-permitting scale, suggesting that local effects of land management are more important than previously thought. In a study by Gutjahr et al. (2016) the spatial variability of extremes increases at 1-km resolution and matches the observations. A comprehensive review of the improvements and deficiencies of convection-permitting simulations is provided by Prein et al. (2015). To date, the application of convection-permitting models in climate studies is limited, and is typically restricted to relatively small domains (Knote et al. 2010; Prein et al. 2013; Tölle et al. 2014; Gutjahr et al. 2016). Often, only a few summer seasons (Hohenegger et al. 2008; Prein et al. 2013; Lind et al. 2016) are investigated because of computational constraints. The immense computational costs are inherent with climate simulations at convection-permitting scale. Efforts are currently ongoing to reduce these computation costs (Brisson et al. 2016).

An open issue that has not been adequately addressed is the degree to which higher horizontal resolution is beneficial for climate simulations (Luca et al. 2012) with regard to climate extremes (Gutjahr et al. 2016). In this study, we address the question of whether and to what extent the new information on extremes achieved with higher resolution is related to the simulated horizontal resolution for the region. The investigation of the effect of increasing resolution on model results is important to provide evidence of the need for such simulations. Our investigations

support these efforts and provide directions for further model development at the convection-permitting scale.

Two different convection-permitting climate simulations are performed with CCLM: one for two 6-year time slices (1970–1975 and 2070–2075), and one for two 10-year time slices (1991–2000 and 2091–2100). Both simulations are forced by the IPCC A1B scenario (IPCC 2007). The simulation domain covers an extended region of Germany (488 km × 489 km; Fig. 1 gray box) for the 6-year time slices and Rhineland-Palatinate (RLP) for the 10-year time slices. These are among the first convection-permitting regional climate simulations over such large domains and for such long periods of time. Previously, CCLM forced by ERA-40 reanalysis data was evaluated for RLP, and showed general agreement with observations at high-resolution scales below 5 km (Gutjahr et al. 2016; Schefczyk and Heinemann 2017).

Our simulations add to the convection-permitting simulations of Gutjahr et al. (2016), and to the range of climate projections for the twenty-first century already available in the literature.

An overview of the model and observational data followed by a description of the analytical procedure used are presented in Section 2. Section 3 contains the analysis for evaluation of the climatology of temperature and precipitation. In particular, the ability of the model to realistically represent climate extremes distributed over the domain is investigated. Furthermore, it is devoted to analyzing the differences due to model resolution of climate changes and their extremes expected under the IPCC A1B greenhouse gas emissions scenario. In Section 4, a summary and the main conclusions are presented.

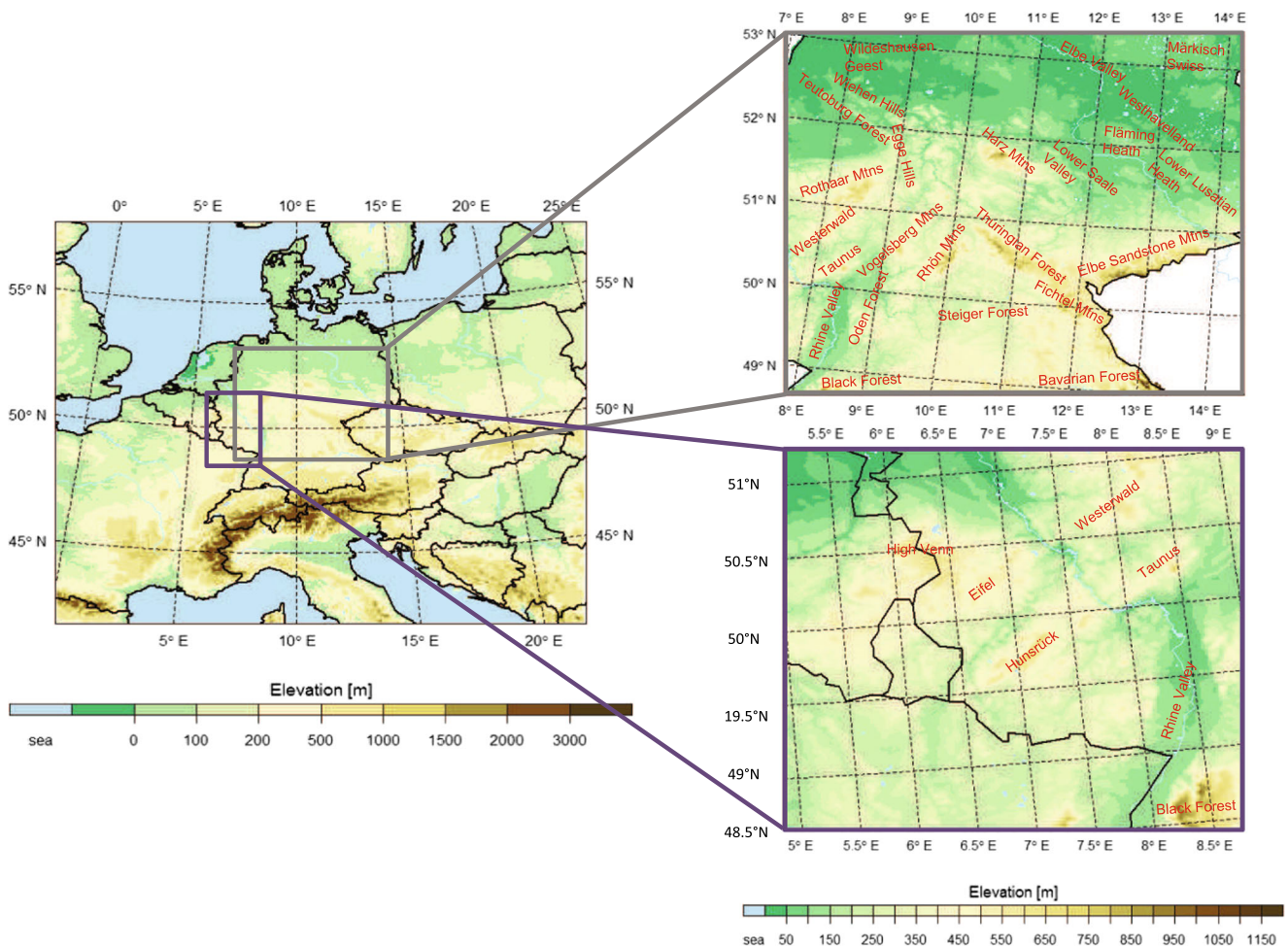


Fig. 1 Simulation domains for the nesting steps and topography [m]. The whole 7-km domain of the convection-parameterizing model (CLM7) is shown on the left. The 1.3-km domain of the convection-permitting model (CLM1) covers Central Germany is highlighted by the gray box (upper-right panel). The domain in the purple

box covers Rhineland-Palatinate, northwest of Baden-Württemberg, parts of France, Luxembourg, Belgium, and the Netherlands for the convection-parameterizing (CLM5RLP) and the convection-permitting (CLM1RLP) models (lower-right panel). Characteristic locations with orographic features are named (Mtns: Mountains)

2 Methods

2.1 Regional model

The regional climate model CCLM, version COSMO4.8_clm17, was employed for climate simulations of historical and future periods. This model is the climate version of the non-hydrostatic limited-area atmospheric prediction model COSMO developed by the German Weather Service (DWD; Stepler et al. 2003) for meso-scale applications (Schättler et al. 2009). A double nesting procedure in rotated coordinates was employed (18 km to 7 km to 1.3 km) by using dynamically downscaled climate IPCC 20C and scenario A1B data (IPCC 2007) of the CCLM at ~ 18 km (0.165° on a rotated grid, Hollweg et al. 2008) as lateral boundary conditions (see Fig. 1). The basis model of the one-way nesting procedure was the GCM ECHAM5/MPI-OM (Roeckner et al. 2006). The coarsest simulated nest at ~ 7 km (0.0625° on a rotated grid) comprised central Europe (254×254 grid points). The finest nest was centered on Germany (375×376 grid points) with ~ 1.3 km (0.0118° on a rotated grid), as indicated by the gray box in Fig. 1. All simulations used 40 vertical atmosphere levels and ten soil layers with a total soil depth of 15.34 m. The number of vertical atmosphere levels represented a compromise between resolution and available computational resources. The lowest 2 km of the atmosphere consisted of 14 layers to capture boundary layer processes sufficiently (Gutjahr et al. 2016). Throughout this paper, the CCLM 18-km resolution simulation is referred to as CLM18, the CCLM 7-km resolution simulation is referred to as CLM7, and the CCLM 1.3-km resolution simulation is referred to as CLM1. The simulations of CLM7 were performed for the years 1970–2000 (control time period) and 2070–2100. Because of the very high computational costs, the highest spatial resolution simulation, CLM1, was employed to simulate only two 6-year time slices (1970–1975 and 2070–2075). The first year of CLM1 was not removed for the spin-up period as warm start simulations were performed. The soil moisture in the coarse resolution model CLM7 was initialized with the soil moisture climatology from the consortial runs. Furthermore, CLM7 was initialized 3 years prior to the analysis periods, which ensured an appropriate spin-up time for soil moisture.

Because a 6-year period was generally considered too short to provide projections, we added the two 10-year simulations at the convection-permitting scale of Gutjahr et al. (2016) driven by the same large-scale forcing for the time periods 1991–2000 (control) versus 2091–2100, but for a smaller domain covering Rhineland-Palatinate and northwest of Baden-Württemberg, as shown in Fig. 1 (purple marked border). Here, the CCLM 4.5-km resolution

simulation (1971–2000 and 2071–2100) is referred to as CLM5RLP, and the CCLM 1.3-km resolution simulation is referred to as CLM1RLP. CLM5RLP was configured with 279×204 horizontal grid boxes and a time step of 45 s at 4.5-km resolution, and CLM1RLP with 220×220 horizontal grid boxes and a time step of 12 s at 1.3 km. The overlapping area with CLM7 and CLM1 was used for analysis during the evaluation period because of the availability of high-resolution observational data. For climate change analysis, the whole domain of RLP was used.

The model relied on the primitive hydro-thermodynamical equations describing compressible non-hydrostatic flow in a moist atmosphere. The CCLM used a Runge-Kutta time-stepping scheme (Wicker and Skamarock 2002) with a fifth-order advection scheme (Doms and Baldauf 2015). The radiation scheme of Ritter and Geleyn (1992) was called every hour in the simulation. The convection scheme by Tiedtke (1989) for convective mass flux parameterization was used in all of the simulations. In CLM7 and CLM5RLP, deep convection was parameterized using the Tiedtke scheme, whereas for CLM1 and CLM1RLP, it was explicitly resolved. Shallow convection of the Tiedtke parameterization was used for the highest resolution simulations as well as subgrid parameterization for turbulent transport in the boundary layer. Prognostic precipitation (including graupel) was calculated with a four-category microphysics scheme (Doms and Baldauf 2015). Vertical turbulent diffusion was calculated from prognostic turbulent kinetic energy (Raschendorfer 2001), including the effects of subgrid-scale condensation and thermal circulation. CCLM was set up in a rotated coordinate system, and the atmospheric model variables were staggered on an Arakawa-C grid (Schättler et al. 2009). The turbulent fluxes were exchanged with the surface through the multi-layer soil model TERRA-ML (Heise et al. 2006). This scheme accounts for infiltration, percolation, capillary movement, melting and freezing of snow, evapotranspiration, and runoff. Plant characteristics and soil types were prescribed from the dominant land characteristics within a given grid box. The spatial distribution of land use was based on the data set of ECOCLIMAP (Champeaux et al. 2005). The Harmonized World Soil Database (HWSD) with a horizontal resolution of 1 km was used for the soil. The external parameters of the orography were extracted from the raw data of GTOPO30 (USGS 1996). These raw data sets were aggregated for the target grid (7/4.5 km and 1.3 km), accounting for all raw data elements within the target grid element using a time invariant data preprocessor (Smiatek et al. 2008).

The model configuration used was reported by Gutjahr et al. (2016). We adapted their configuration and downscaling procedure for an extended model domain. Several studies (e.g., Ban et al. 2014; Fossier et al. 2015)

Table 1 Model configuration and downscaling steps

Model parameter	2nd nesting	3rd nesting
Model	CLM7/CLM5RLP	CLM1/CLM1RLP
Grid resolution	0.0625° ~ 7 km/0.025° ~ 4.5 km	0.0118° ~ 1.3 km
Forcing	CCLM ~ 18 km	CCLM ~ 7 km/CCLM ~ 4.5 km
N. of grid points	254 × 254/279 × 204	375 × 375/220 × 220
Model time step	45 s	12 s
Integration scheme	Runge-Kutta	Runge-Kutta
Atmospheric layers	40	40
Convection scheme	Tiedtke, Graupel	Shallow convection, Graupel
Greenhouse gas forcing	C20 and A1B IPCC-SRES control and emission scenarios (run 1)	

The complete 3D RCM consists of two parts: the atmospheric model COSMO-CLM and the land-surface module TERRA-ML (Tölle et al. 2014; Gutjahr et al. 2016)

employed similar simulation experiments to examine the benefits of convection-permitting simulations. The model configurations for all our four simulations were similar except for their model resolutions, domains, and time steps (see Table 1). The main difference to the coarser resolution models was that the deep convection scheme was turned off in both 1.3-km simulations, and the simulations of RLP were carried out with an older version of the model (COSMO4.8.clm11), but with no significant changes. Because the present study investigated improvements and limitations in the representation of climate changes and extremes resulting from increased horizontal resolution, the main focus was the analysis of CLM7, CLM1, CLM5RLP, and CLM1RLP.

2.2 Model domain

The orography of the simulation domains is shown in Fig. 1. The topography of CLM1 and names of characteristic orographic features of the model domain of mid Germany are shown in the upper-right panel. In the lower-right panel, the area of RLP is indicated. Both represent the domains for the analysis described herein. The topography is dominated by large, relatively flat areas, including the Wildhausen Geest in the northwest, the Rhine Valley in the southwest, the Elbe Valley and Westhavelland in the northeast, and the Lower Saale Valley in the central east. Clearly visible in the topography of the highest resolution simulation CLM1 are the hill formations in the middle of the domain that cover the Rothaar Mountains, with the Langenberg (843 m) in the west, the Harz Mountains with the Brocken (1141 m) in the center, and the mountain ranges (Grosser Beerberg, 982 m) of the Thuringian Forest in the east of Germany. In addition, river valleys and small to medium-sized lakes in northeastern Germany are distinctly different from CLM7. The presence of small gradients in the topography becomes

apparent. These changes in topography with higher resolution have considerable influence on orographic convection and temperature.

2.3 Observational data sets

Because one of the aims of our study was to analyze the benefits of increasing resolution on extreme temperature and precipitation fields, observational data sets with higher resolution than the model results would be preferable. However, the standard reference gridded data set of air temperature and precipitation at daily resolution covering all of Europe was E-OBS (Haylock et al. 2008), which is resolved at 25 km. Therefore, the daily gridded data set HYRAS (Frick et al. 2014), provided by the German Weather Service, was used for evaluation. HYRAS consists of data from about 2000 weather stations. These data were spatially interpolated onto a 1-km grid using the REGNIE (“REGionalisierte NIEderschlagshöhe”, engl. Regionalized precipitation amount) method (Rauthe et al. 2013). In this study, the original gridded observational values at 1-km spatial extents for temperature and precipitation were used for comparison.

The simulation results were remapped on the observed grid using a bilinear interpolation method that allowed the observed data (considered the “true” data) to be retained unaltered. Thus, the high-resolution climate features, which are of primary interest for our purposes, are maintained. With this procedure, a grid-cell-wise comparison was possible, and potential improvements caused by varying the RCM resolution could be detected. If the comparison was made with lower-resolution data sets, many features of the finer-resolution simulations would have been smoothed out (Vautard et al. 2013). Although Kotlarski et al. (2014) recommended interpolation to the coarsest-resolution grid, we employed the first approach to provide information for

impact studies, as supported by Zollo et al. (2015). This method allowed preservation of extreme values and temporal variability (Vautard et al. 2013). The supporting information (Figures S1–S3) provides example references for the effects of upscaling to the coarsest resolution and downscaling to the highest resolution for the region considered. Here, the simulation results were upgraded/downgraded to the resolution of the coarsest/finest-scale RCMs. The differences between the upgraded/downgraded results and the RCM output with no scaling indicated the effects on temperature and precipitation changes and how they were resolved at the different model scales.

2.4 Statistical analysis

In the evaluation period, the climate simulations were compared with the HYRAS observational data set over time periods defined according to data availability. Commonly used performance indices were applied for evaluation. Statistics of mean monthly bias (Model - Observation), standard deviation (SD) and root mean square error (RMSE) averaged over the area were used to evaluate the results. The spatial agreement between the model and observations was quantitatively evaluated by determining the pattern correlation between observed and simulated fields, as described by Walsh and McGregor (1997). These three statistical parameters (SD, RMSE, and correlation) were graphically summarized in Taylor diagrams.

We adopted a subset of climate indices based on percentile thresholds (e.g., Tank et al. 2009), which are specific to sites, for the analysis of extremes (see also definitions by the Expert Team on Climate Change Detection and Indices (ETCCDI) for details).

For the evaluation with observations the procedure was as follows. Due to unavailability of daily maximum temperature observations for the evaluation analysis, TX90p was estimated from daily temperature values of HYRAS and model data for the reference period, and was then named T90p. Here, the data were normalized prior to analysis by subtracting their mean and dividing by their standard deviation. The 90th percentile threshold to calculate T90p was based on the domain median 90th percentile of the observations.

R95pTOT and R99pTOT (Tank et al. 2009; Herrera et al. 2010) constitute the percentages of extreme events, exceeding the 95% and 99% percentiles of the reference period, on the total precipitation.

To analyze projected changes in extreme climate events, we calculated maximum temperature and both precipitation indices based on the whole distribution, and based on summer and winter days. These indices were then expressed as anomalies relative to the local climate. TX90p was the percentage of days when the maximum temperature exceeded

the 90th percentile of the reference period. R95pTOT and R99pTOT were the percentages of total precipitation associated with events with precipitation higher than the 95th and 99th percentiles, respectively, for the reference period. Note that all days, not only wet days, were considered to avoid substantial biases, as discussed by Ban et al. (2015).

The regional climate change signals between the historical and future periods (difference between the time periods 2070–2075 and 1970–1975, and between 2091–2000 and 1991–2000) were calculated for the winter and summer seasons. We then compared the climate change signals between the models to demonstrate the differences caused by spatial scale effects. The significance of the projected changes in each simulation was analyzed by applying a modified Student's *t*-test (two-sided) to seasonal averages following the methodology of von Storch and Zwiers (1999). Because the variance of an autocorrelated time series is smaller than that of an uncorrelated series, the standard *t* statistic would be overestimated. Consequently, the null hypothesis (the mean values of the time series are equal) would be more frequently rejected than it should be. In the modified method, the use of permutations was applied to reduce the number of false rejections of the null hypothesis by accounting for time dependence within the series. Significant areas for a two-sided test at the 0.05 significance level were hatched in the figures. If the whole area was significant, it was documented in the figure label, and the hatching was left out. For the box-and-whisker plots, a non-parametric, two-sided Mann-Whitney *U* test was applied for significance testing with $\alpha = 5\%$.

3 Results

3.1 Climate evaluation of precipitation

The analysis of the seasonal representation of the spatial distribution of precipitation across the domain relative to HYRAS is presented in Fig. 2 for CLM7 and CLM1 over the time period 1970–1975, for the winter (DJF) and summer (JJA) seasons. Although CCLM is generally able to represent the overall spatial distribution of seasonal mean daily precipitation, both simulations overestimate summer and winter precipitation compared to the observations, predominantly over mountainous areas. The domain-averaged wet bias of both simulations is largest in summer (about 1.66 mm/day for CLM7, about 1.41 mm/day for CLM1), and smaller in winter (about 0.96 mm/day for CLM7, about 0.73 mm/day for CLM1). The wet bias reduces in CLM1 compared with CLM7 for both seasons. That CLM1 is drier than CLM7 in summer indicates lowered convective activity. In CLM1 deep convection parameterization is switched off, but shallow convection is still active. The shallow

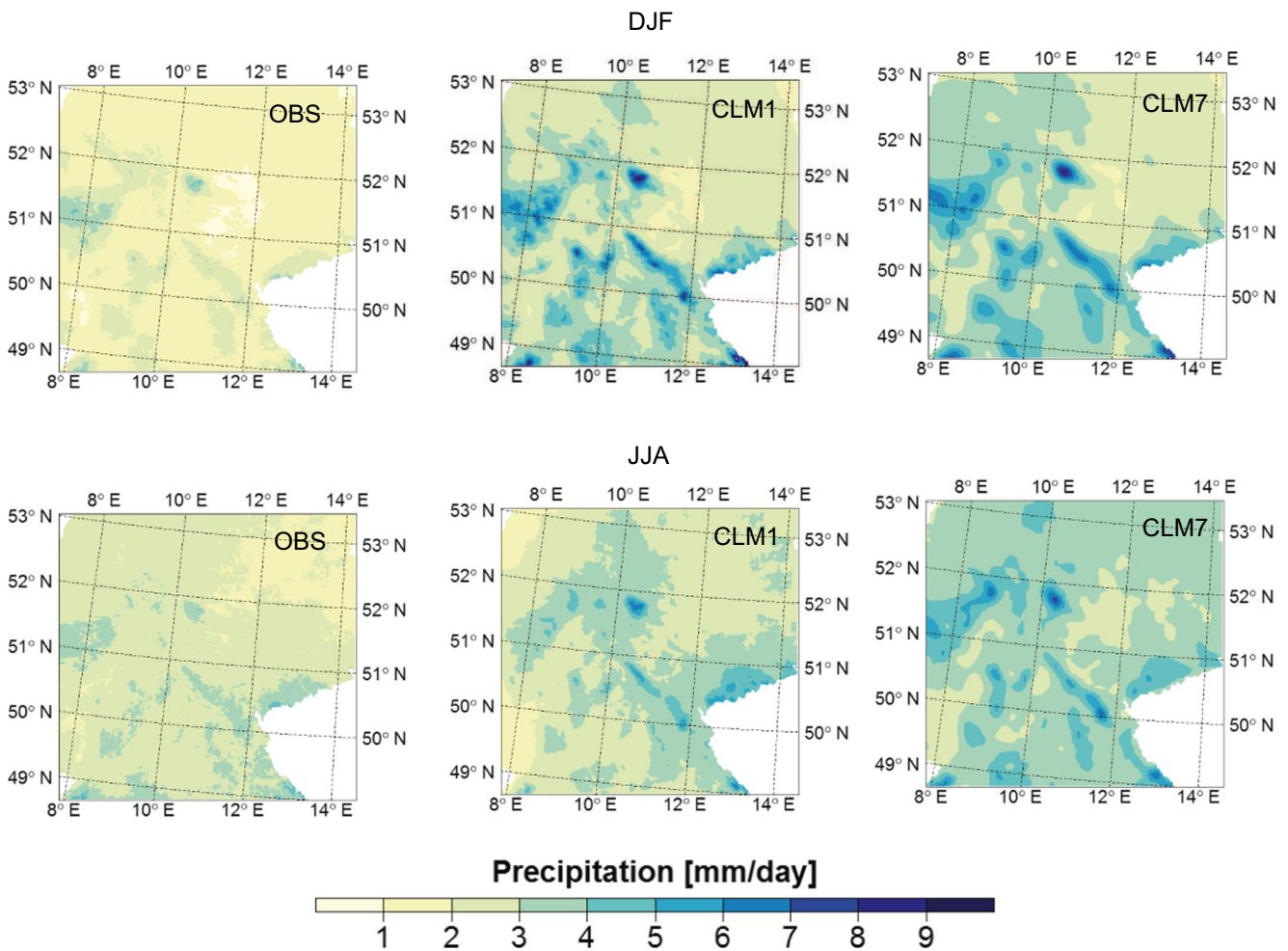


Fig. 2 Spatial distribution of daily mean precipitation [mm/day] for (top) winter (DJF) and (bottom) summer (JJA) seasons obtained for the German Meteorological Service observations (HYRAS named OBS) and COSMO-CLM simulations (CLM1 and CLM7) averaged over the time period 1970–1975

convection scheme may be too aggressive at this high resolution (pers. comm. U. Blahak from the German Weather Service). Consequently, the convection layer is stabilized, which prevents convective development and precipitation. It may be interesting to decrease the thickness of the shallow convection layer in the model, as well as the entrainment rate for shallow convection, in further simulation experiments or to switch it off entirely. These results show that precipitation is particularly sensitive to the selected convection scheme. However, the resolution between 4 and 7 km is a gray zone (Prein et al. 2015), where convection is partly resolved and partly parameterized. The enhanced precipitation in CLM7 might thus be caused by too strong deep convection (Prein et al. 2013).

Berg et al. (2013) obtained an overestimation of precipitation in their 7-km simulation with CCLM over the whole of Germany, but for a 30 year time period. In that study, downscaling was performed using a different double nesting approach (200 km to 50 km to 7 km). These findings

suggest that the bias of the coarse resolution simulation is passed unchanged to the nesting simulation. When the same air mass of the coarse resolution model is driven over the higher topography of CLM7 or CLM1, significantly more precipitation is generated by orographic uplift, e.g. in the Rothaar and Harz Mountains, or in the Thuringian Forest. It is a well-known problem that RCMs produce too much precipitation over mountainous areas (e.g., Ban et al. 2014; Lind et al. 2016). With higher spatial resolution, the orography is more pronounced. Mountain ranges block large-scale atmospheric flow and generate orographic rainfall, which contributes to the wet bias. It is worth noting that errors in precipitation observations may contribute to these biases over the mountainous areas, as these errors increase at high altitudes (Bucchignani et al. 2016).

Furthermore, the two model runs overestimate precipitation over the dry lowlands of northern Germany, especially in summer. The orographically complex terrain does not explain the inconsistencies here because the northern area is

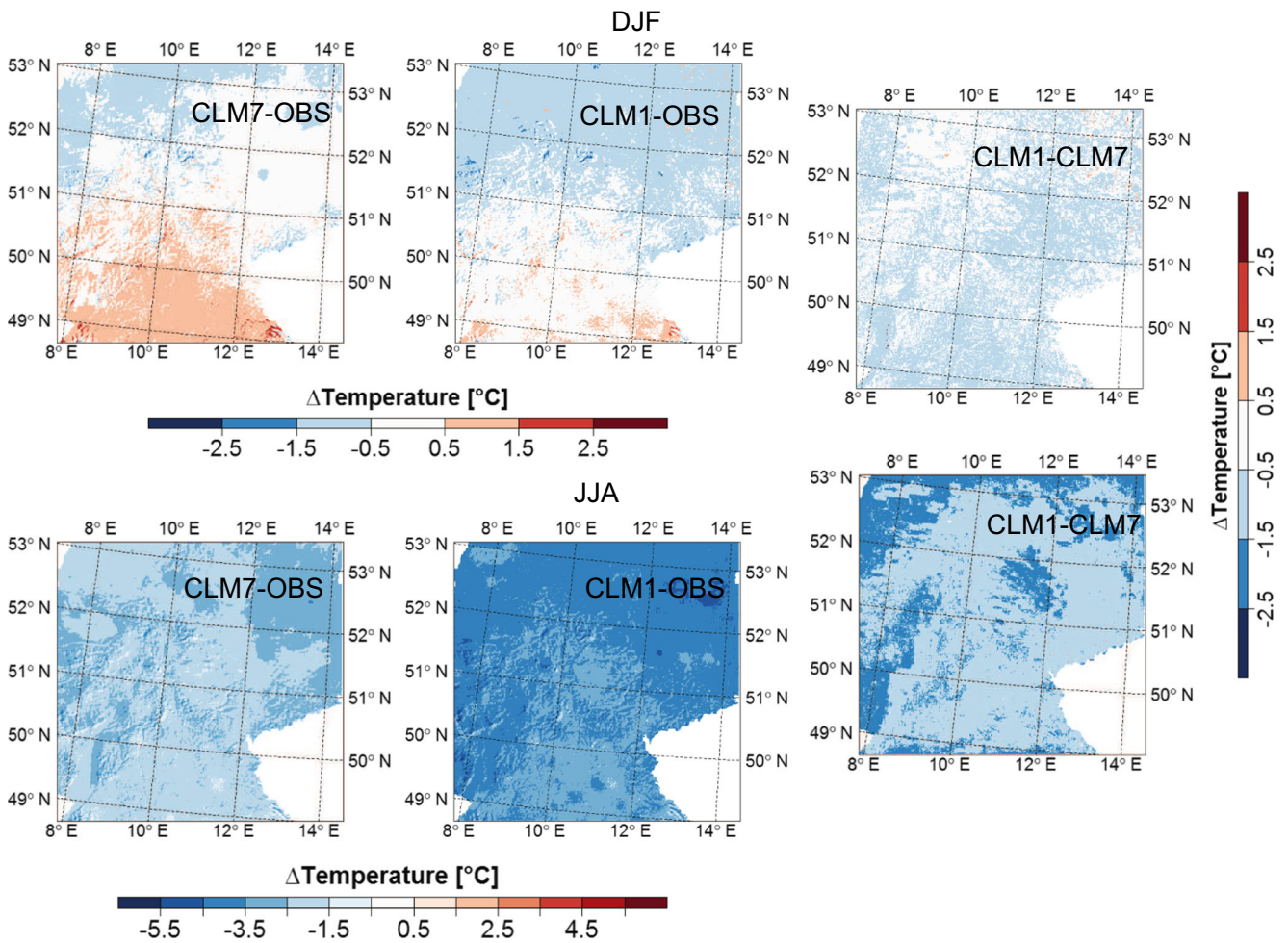
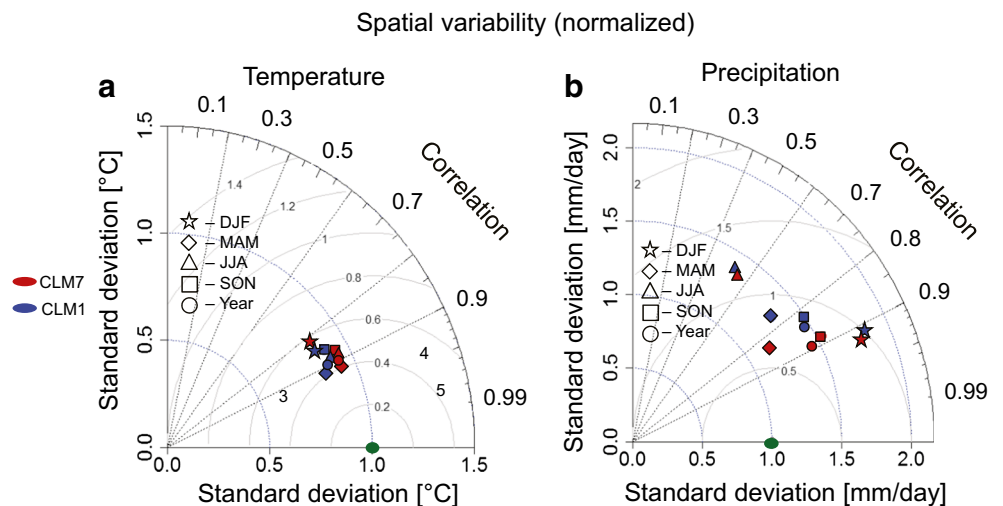


Fig. 3 Spatial distribution of mean temperature bias for (top) winter (DecFeb (DJF)) and (bottom) summer (JunAug (JJA)) seasons for (left column) the convection-parameterizing model (CLM7), (middle column) the convectionpermitting model (CLM1), and (right column) the difference between the two (CLM1 minus CLM7) averaged over the

time period 19701975. The height correction applied to account for topographic differences (between model and observations and between models) assumes a lapse rate of 0.65 K/100 m. Note the different color bar for CLM1 minus CLM7. The bias is evaluated against HYRAS (OBS)

Fig. 4 Taylor diagram of the COSMO-CLM simulations (CLM1 (blue) and CLM7 (red)) with HYRAS observations (green) for temperature (left panel) and precipitation (right panel) showing pattern correlations (black dotted lines), centered RMS errors (gray contours), and normalized standard deviations (blue dotted lines). DJF: Dec–Feb, MAM: Mar–May, JJA: Jun–Aug, SON: Sep–Nov



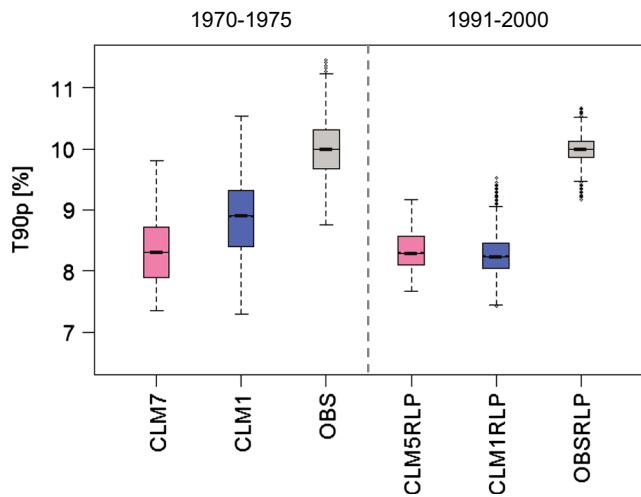


Fig. 5 Spatial distribution of T90p summarized as box plots for simulation chains CLM7-CLM1 (left side), and CLM5RLP-CLM1RLP (right side) compared with HYRAS observations. The evaluation period for CLM7 and CLM1 is 1970–1975, and for CLM5RLP and CLM1RLP it is 1991–2000. Differences are significant at the 0.001 level

flat. Berg et al. (2009) showed that the availability of moisture is the dominant factor for precipitation during summer, which is related to the soil texture. Warrach-Sagi et al. (2013) attributed the overestimation of precipitation over

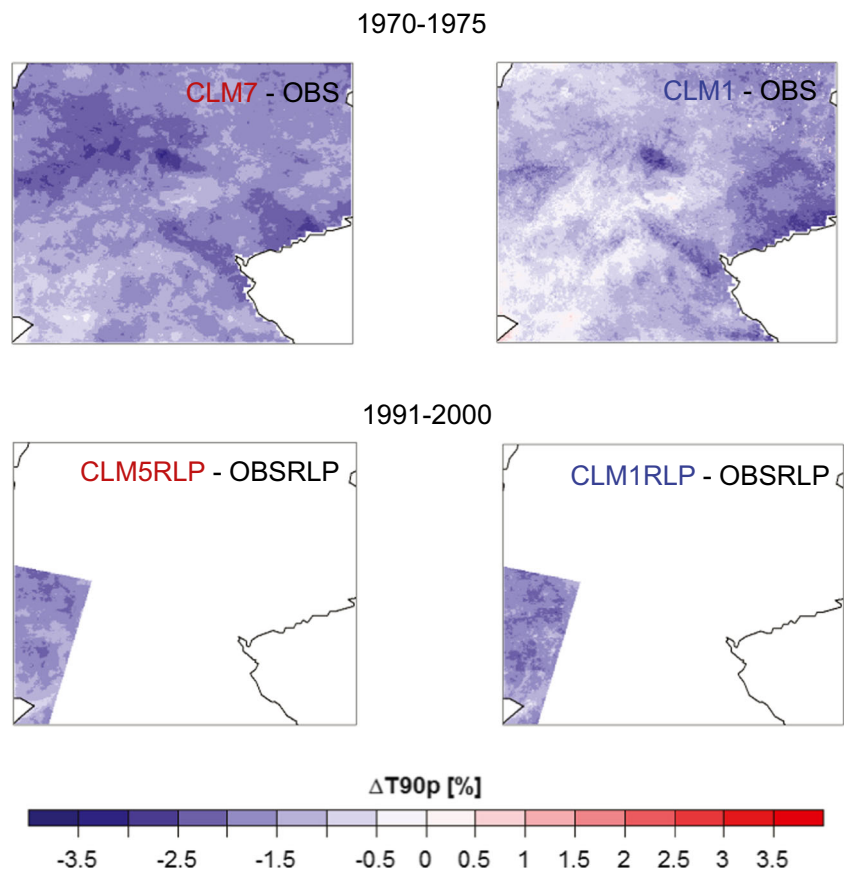
the northern region to the soil data of the regional climate model. CCLM assumes loamy soils in northern Germany, although sandy soils are dominant in nature (Warrach-Sagi et al. 2013). Even though the results show distinct biases relative to the observations, the differences are within the range of model errors depicted by Jacob et al. (2012).

3.2 Climate evaluation of temperature

Spatial distribution biases of simulated 2-m temperatures of CLM7 and CLM1 are compared with the HYRAS data set averaged over the time period 1970–1975, considering the winter (DJF) and summer (JJA) seasons (Fig. 3, left and middle columns). The difference between CLM1 and CLM7 is shown in the third right column.

In the winter season, a cold bias (up to 1.5 °C) is found over most of the northern domain in both models (Fig. 3, upper left and middle columns). A warm bias is apparent in the southern domain. The warm bias is weaker and the cold bias stronger in the CLM1 simulation than in CLM7. The largest biases are found over mountain ranges in both models, but these biases are weaker in magnitude in CLM1. Such a cold bias during the winter season has also been reported by Ban et al. (2014). Overestimating precipitation at high altitudes (see Fig. 2) can lead to temperature

Fig. 6 Differences in spatial distribution relative to HYRAS observations of T90p over the domain for simulation chains CLM7-CLM1 (upper panel), and CLM5RLP-CLM1RLP (lower panel). The evaluation period is the same as in Fig. 5



underestimations, as demonstrated by Haslinger et al. (2013). Furthermore, cold biases are apparent over urban areas. An urban module is not included in these simulations. Therefore, the model is not able to represent urban heat islands that become more relevant in CLM1. Furthermore, CLM1 is warmer than CLM7 over lakes and rivers. This finding is also visible in the difference between CLM1 and HYRAS. Here, again, the simulations were conducted without an explicit lake module.

The cold bias of the models in the summer season is stronger in CLM1 (3–4 °C) than in CLM7 (2–3 °C) (Fig. 3, lower left and middle columns). Differences between the two models (CLM1 and CLM7) are small in winter (up to 1.5 °C) and more distinct in summer (up to 2.5 °C) (Fig. 3 right panel). The greatest differences occur over the large, flat agricultural areas (as indicated in Fig. 1 right panel), where CLM1 is colder than CLM7. We suggest that these differences are caused by the parameterization of the planetary boundary, which was not adjusted in CLM1. We assumed a large asymptotic turbulent length scale of 500 m in CLM1 in the planetary boundary layer scheme, which is not modified compared with CLM7. This difference may lead to lower air temperatures and thus to an enhanced cold bias because of enhanced vertical mixing (Ban et al. 2014). This assumption is supported by the reduced amounts of precipitation in CLM1 apparent in Fig. 2. Another reason for the discrepancies may be that the calling frequency of the radiation scheme (every hour) was too low. Several studies (e.g., Hohenegger et al. 2009; Froidevaux et al. 2014) have demonstrated that physical feedback processes become more relevant with higher resolution. Accordingly, greater biases are apparent at higher resolution in summer if these processes are not accounted for. Therefore, the resulting differences rely on the strength of the interaction between subgrid-scale moisture and atmospheric temperature anomalies. The mean summer bias of CCLM over Germany for the period 1961–2000 (Jacob et al. 2012) is comparable with the cold bias of our simulations. This finding suggests that in addition to the known problems of a cold summer bias in CCLM, using ECHAM5/MPI-OM as boundary forcing may introduce additional biases from potentially erroneous global forcing, as most GCMs tend to underestimate temperature (Macadam et al. 2010). Further studies are needed to test which configuration is optimal for convection-permitting simulations. In addition, erroneous spatial interpolation of observation data must be addressed.

3.3 Analysis of Taylor plots

Normalized Taylor plots are presented in Fig. 4 to illustrate the spatial variability of seasonal and annual temperature

and precipitation compared with HYRAS based on daily values.

3.3.1 Temperature

CLM1 and CLM7 reproduce similar temperature distributions (Fig. 4 a), which indicates that the 7-km model sufficiently resolves the spatial variability. The standard deviations for both models are smaller (0.7–0.9) than those of the observations. CLM1 and CLM7 show remarkable similarity in their RMSEs. The difference between the simulations compared with the observations becomes apparent in the pattern correlation analysis. Although small, improvements are seen for CLM1 throughout the year. CLM7 has slightly weaker spatial correlation (about 0.01–0.03 less than CLM1), even though this simulation is not very different from CLM1. CLM1 captures the very fine-scale variability of temperature because of its finer resolution of the orographic and land-surface gradients. As pointed out by Kotlarski et al. (2005), the use of fine horizontal resolution is expected to allow more realistic representation of orographically controlled local meteorological features.

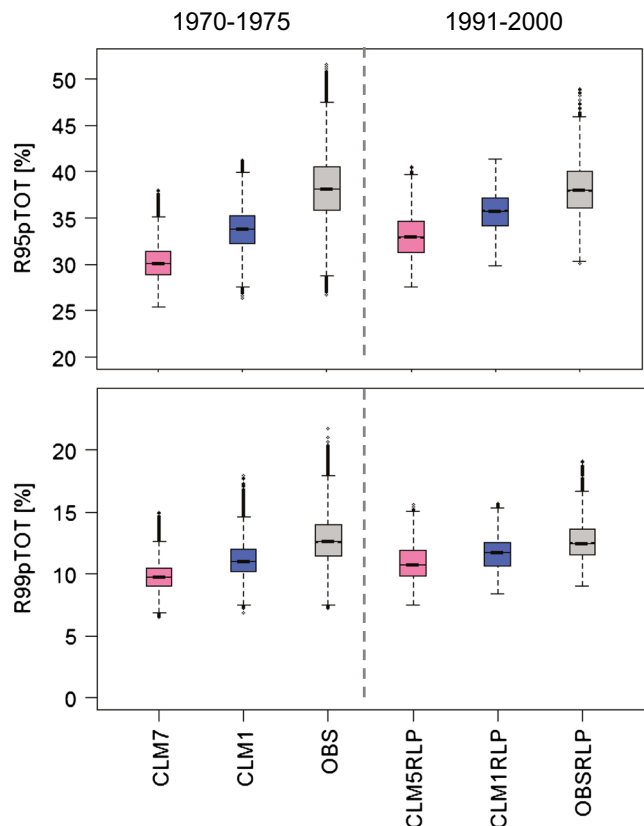


Fig. 7 Spatial distributions summarized as box plots of R95pTOT (upper panel), R99pTOT (lower panel) for simulation chains CLM7-CLM1 (left column) and CLM5RLP-CLM1RLP (right column) compared with HYRAS observations. Differences are significant at the 0.001 level. The evaluation period is the same as in Fig. 5

3.3.2 Precipitation

All of the simulations overestimate precipitation amounts in winter and autumn. CLM1 shows minor improvement in performance relative to CLM7 (Fig. 4b). Lower pattern correlations (~ 0.5) are detected for the summer season, which is characterized by higher rainfall rates at small spatial clusters. Correlations are highest for the winter season (~ 0.91 – 0.93). The agreement across resolutions may be attributed to the already relatively high resolution of CLM7 (Fosser et al. 2016). In contrast with our findings, Kendon et al. (2014) and Ban et al. (2015) reported improvements in their convection-permitting simulations at 2-km resolution, especially in summer, compared with the convection-parameterized model at 12-km resolution.

3.4 Climate evaluation of temperature extremes

The spatial distribution of T90p is summarized in Fig. 5 as box plots for model chains CLM7-CLM1 and CLM5RLP-CLM1RLP relative to observations. The evaluation period for CLM7 and CLM1 is 1970–1975, and for CLM5RLP and CLM1RLP, it is 1991–2000, based on data availability. Here, T90p represents the percentage of exceedance over the median 90th percentile of the observations for the domain. In both simulation chains, the median is improved toward the observations with increasing resolution, although for CLM1RLP, this improvement is less prominent because of the smaller model domain. All simulations tend to overestimate the observed variability indicated by the higher spatial variance. The largest discrepancies relative to observational temperature extremes

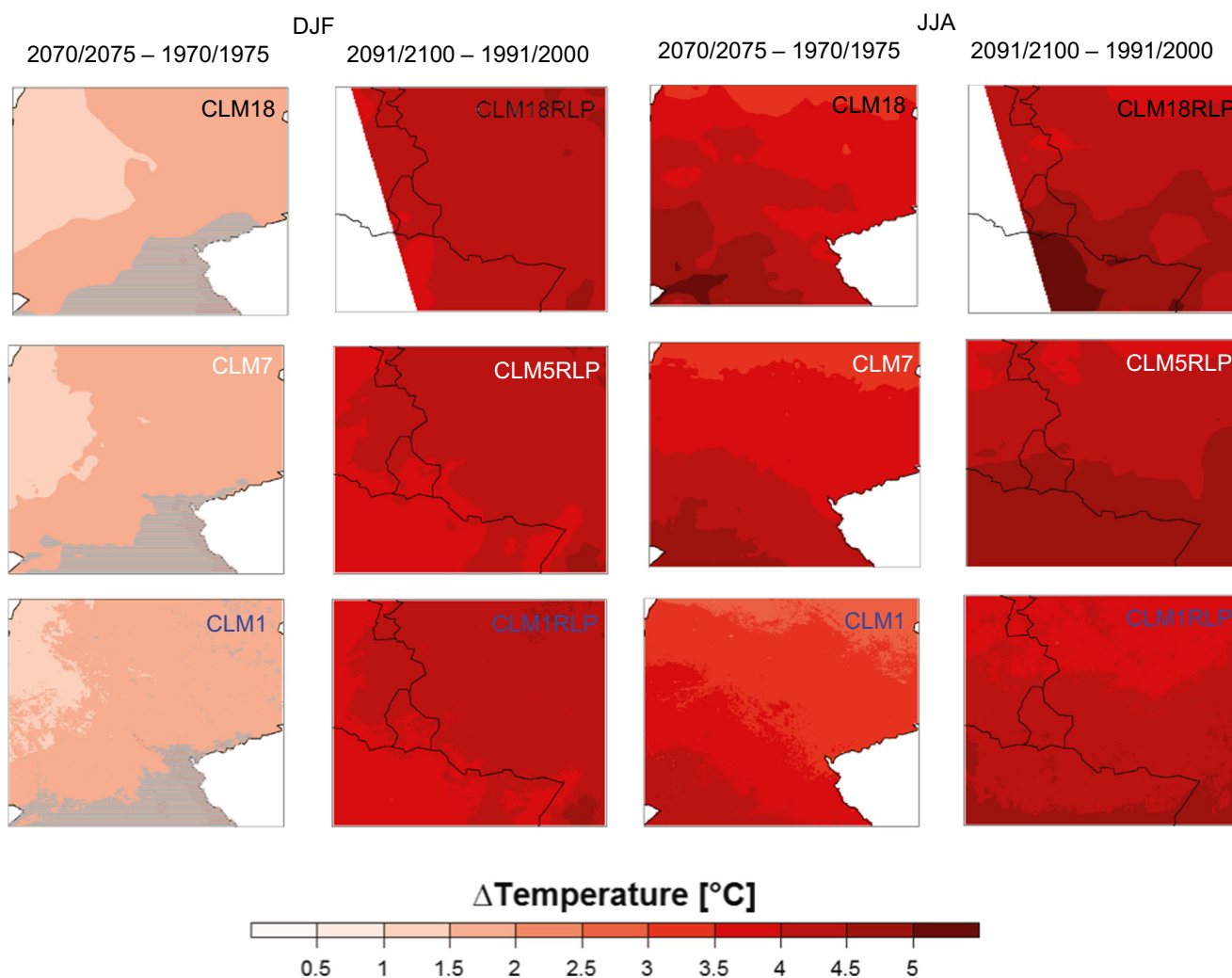


Fig. 8 Spatial distribution of the climate change signal in mean seasonal temperature based on monthly values for each model for winter (left) and summer (right). The climate change period for CLM7 and CLM1 is 2070–2075 versus 1970–1975, and for CLM5RLP and CLM1RLP it is 2091–2100 versus 1991–2000. Hatched areas are

regions where changes are statistically significant at the 0.05 level. All grid points are significant for summer leaving out the hatching. Note that we only show CLM18RLP results for Germany. See Fig. 4 for abbreviations

are found over mountain ranges in both model chains, as represented by distribution differences of T90p over the domain in Fig. 6. The observations show higher values of T90p over the Harz, Rothaar, and Elb Sandstone Mountains, and over the Thuringian Forest. CLM7 and CLM5RLP cannot reproduce this spatial distribution of T90p, although CLM1 and CLM1RLP achieve spatial distributions of T90p much closer to the observations. Precipitation is overestimated at high altitudes, as shown in Fig. 2, which leads to underestimation of temperature in the simulations (see Fig. 3). Furthermore, higher temperatures are also underestimated, and thus temperature extremes are misrepresented. Montesarchio et al. (2014) also found no improvements in extreme temperatures over mountainous areas with the same model, but with a coarser resolution over a different area. These findings suggest that in addition to increasing resolution to convection-permitting scale, parameterizations

must be adapted accordingly. Note that the spatial interpolation of station data in mountainous areas is prone to errors. Interpolation of observational station data from valleys may result in warmer temperatures at mountain tops. This uncertainty also depends on the density of the observational stations.

3.5 Climate evaluation of precipitation extremes

The spatial distributions of R95pTOT and R99pTOT for both model chains (CLM7-CLM1 and CLM5RLP-CLM1RLP) are summarized as box plots in Fig. 7. In both model chains (CLM7-CLM1 and CLM5RLP-CLM1RLP), extreme precipitation values improve toward the observations with increased resolution for both evaluation periods, 1970–1975 and 1991–2000. The medians of the high-resolution simulations (CLM1, CLM1RLP) have much

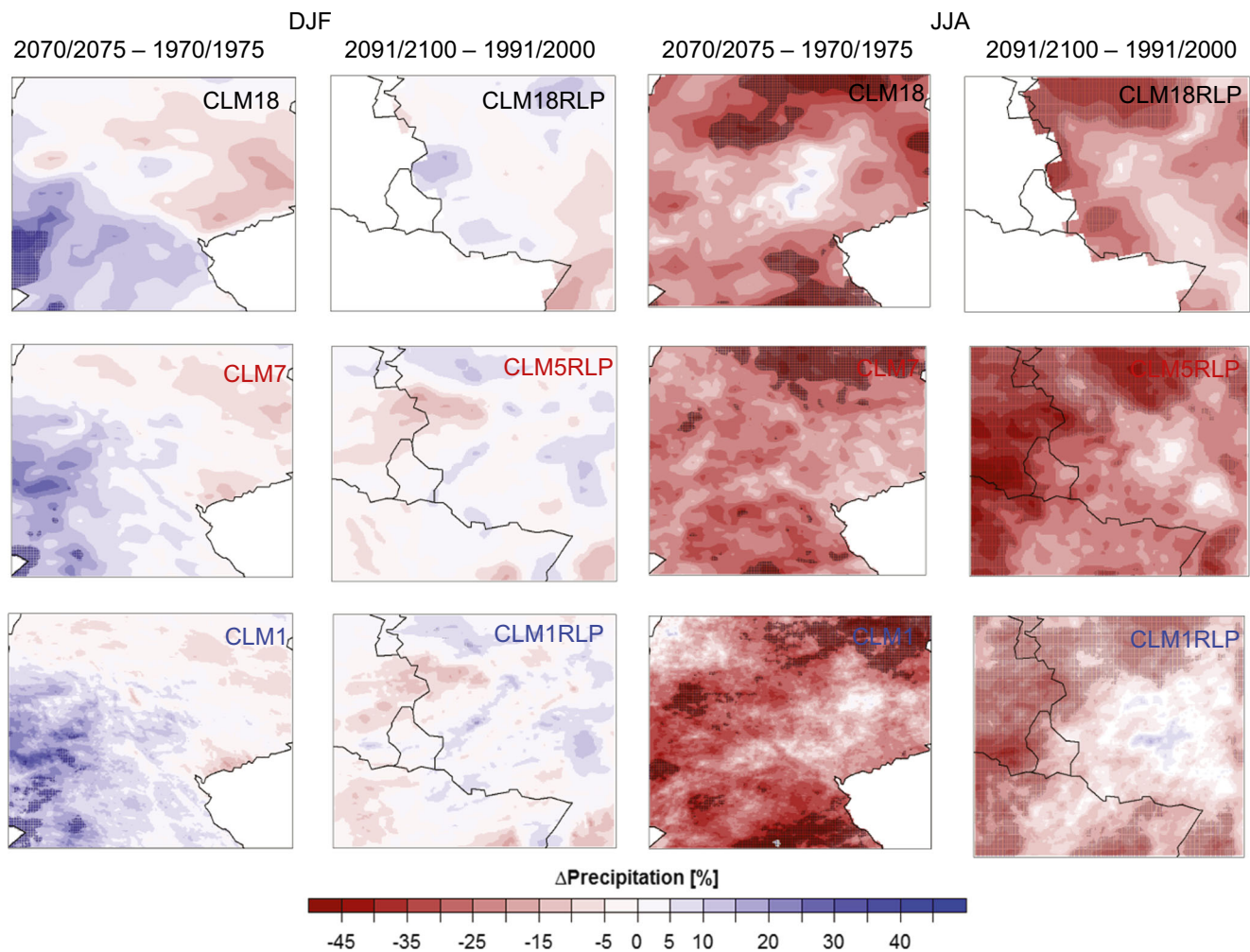


Fig. 9 Spatial distribution of the climate change signal in mean seasonal precipitation based on monthly sums for each model as a percentage for winter (left) and summer (right). The climate change period for CLM7 and CLM1 is 2070–2075 versus 1970–1975, and

for CLM5RLP and CLM1RLP it is 2091–2100 versus 1991–2000. Hatched areas are regions where changes are statistically significant at the 0.05 level. Note that we only show CLM18RLP results for Germany. See Fig. 4 for abbreviations

greater realism for R95pTOT and R99pTOT compared with CLM7 and CLM5RLP. That the CCLM is capable of simulating extremes close to observations at different convection-permitting scales was also demonstrated by Gutjahr et al. (2016). An alternative representation of the results is provided in Figures S4 and S5 of the [Supplementary Material](#) as distributions of R95pTOT and R99pTOT over the domain, showing that the distributions of precipitation extremes are realistically simulated. The amounts of extreme precipitation are lower over mountainous areas for R95pTOT and R99pTOT for all of the simulations and the observations, and are enhanced in the lowlands. However, the models fail to simulate the observed magnitude of extreme precipitation.

3.6 Climate change analysis

The second aim of this work is to investigate the dependence of the development of modeled future atmospheric conditions on model resolution and to provide high-resolution climate projections for Germany in the 21st century by employing the IPCC A1B scenario.

3.6.1 Temperature

Figure 8 shows the change in mean seasonal temperature for the period 2070–2075 with respect to 1970–1975 for mid Germany, and for the period 2091–2100 with respect to 1991–2000 for RLP for winter and summer. The results are shown only according to data availability. Generally, an increase in temperature of about 3 °C is simulated in all seasons over the simulation domain. Peaks of +4 °C to +5 °C are projected over the Black Forest in the southwest in summer. Similar results were found by Jacob et al. (2012), who compared ENSEMBLES simulations for a similar region of Germany. Differences ranged from about 2.5 to 4 °C. The changes shown in Fig. 8 are within the spread seen in these projects. These findings suggest that our results, which are based on one model, are well within the uncertainty of state-of-the-art RCMs. Although the overall patterns of warming are largely similar between our simulations for all seasons, some deviations are apparent. The warming is larger in CLM18 compared with CLM7, whereas CLM1 simulates the least warming. In summer, CLM1 simulates 1 °C less warming than CLM18 or CLM7. CLM1 shows more

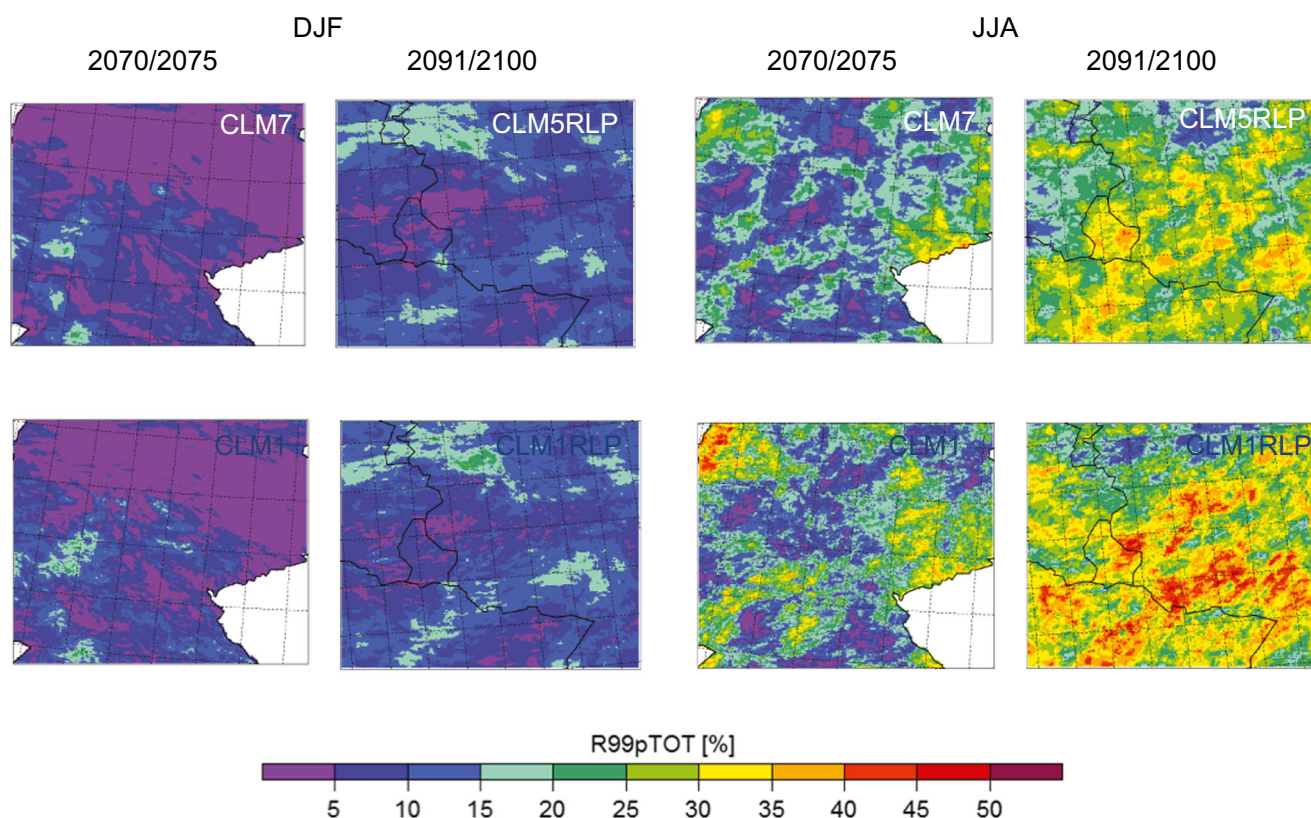


Fig. 10 Spatial distribution of seasonal future climate change of R99pTOT as a percentage change of seasonal total precipitation associated with events with precipitation higher than the 99th percentile of the base period for COSMO-CLM simulation chains CLM7-CLM1

(first and third column), and CLM5RLP-CLM1RLP (second and fourth column). The base period for CLM7 and CLM1 is 1970–1975, and for CLM5RLP and CLM1RLP it is 1991–2000. See Fig. 4 for abbreviations

spatial structure in the signal in all seasons. Similar results are found for the model chain CLM18RLP-CLM5RLP-CLM1RLP.

3.6.2 Precipitation

All precipitation projections show a general decrease in precipitation in summer (see climate change signal for the period 2070–2075 with respect to 1970–1975, and for the period 2091–2010 with respect to 1991–2000 in Fig. 9). Increases in precipitation become more apparent and enhanced over the southern area of Germany in winter. The general precipitation projections agree qualitatively with those of Jacob et al. (2012).

CLM1/CLM1RLP simulates similar changes to CLM7/CLM5RLP, but with more spatial structure and often larger maximums. Differences between resolutions are most apparent in summer. CLM18 projects a minor increase in precipitation southeast of the Harz Mountains. However, CLM7 and CLM1 show a decrease in the precipitation amount. Further, both models simulate enhanced spatial variability, in particular CLM1. Another example is the difference over the RLP domain in summer. CLM18RLP projects a decrease in precipitation in the center of the

domain. Although both, CLM5RLP and CLM1RLP, project an precipitation increase of 5% to 10%, the signals are not significant. Thus, changes associated with model resolution can be strong enough to convert a precipitation increase/decrease into a decrease/increase at higher resolution. Tselioudis et al. (2012) showed that precipitation was produced in higher-resolution models that was not present in the driving model. Much of this precipitation could be attributed to the influence of preceding mountain ranges blocking moisture flow. This process would cause incoming air masses to begin to rise farther from the mountains and, consequently, cause rain to fall farther away (Evans and McCabe 2013).

3.7 Extreme indices

How model resolution affects the projected extremes of temperature and precipitation is of interest. Gutjahr et al. (2016) state that CLM18 is too coarse for extreme value statistics at the local scale. Therefore, we proceed with the analysis of the projected results of CLM7 and CLM1. Results from the simulations of CLM7, CLM1, CLM5RLP, and CLM1RLP are shown only according to data availability. We consider the future period 2070–2075 with respect to the past

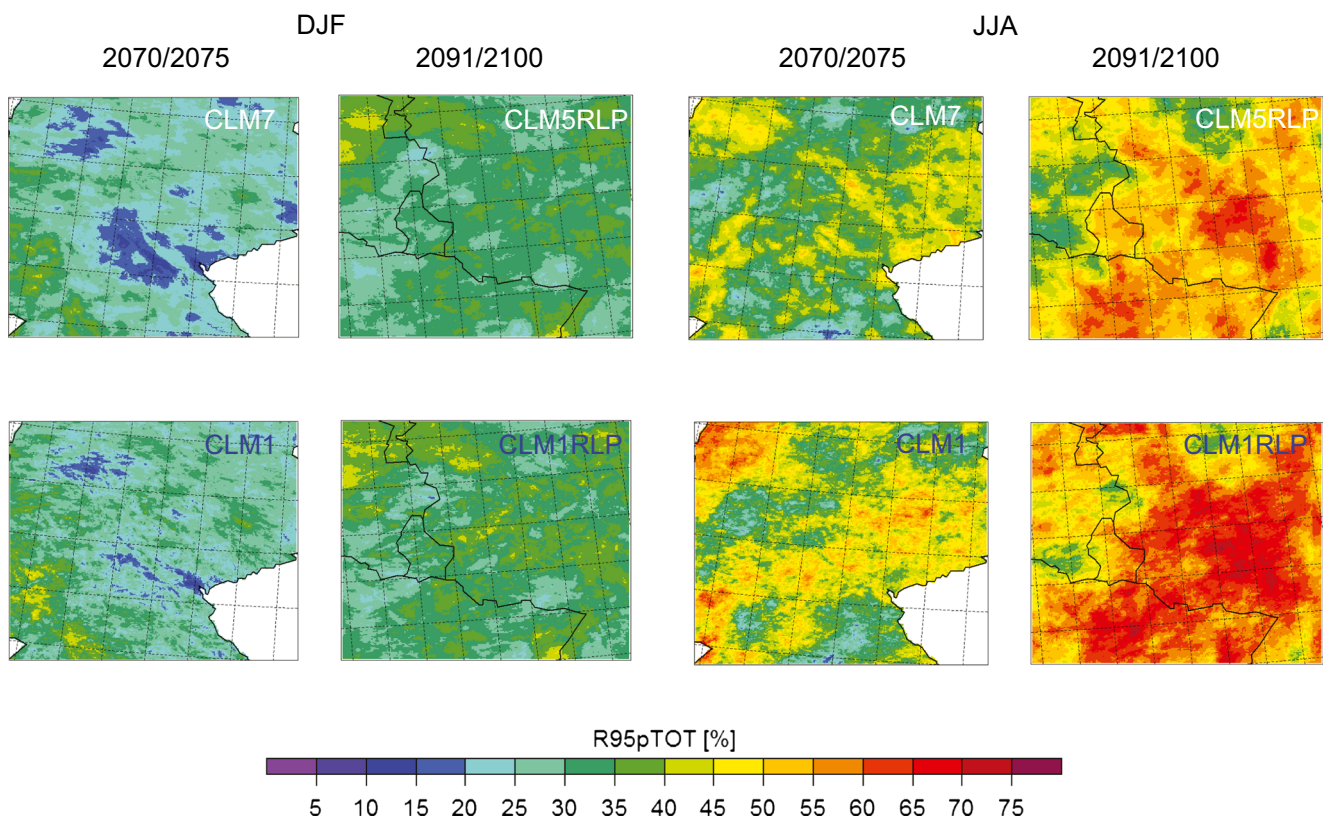


Fig. 11 Spatial distribution of seasonal future climate change of R95pTOT as a percentage change of seasonal total precipitation due to events with precipitation higher than the 95th percentile of the base period for COSMO-CLM simulation chains CLM7-CLM1 (first

and third column), and CLM5RLP-CLM1RLP (second and fourth column). The base period for CLM7 and CLM1 is 1970–1975, and for CLM5RLP and CLM1RLP it is 1991–2000. See Fig. 4 for abbreviations

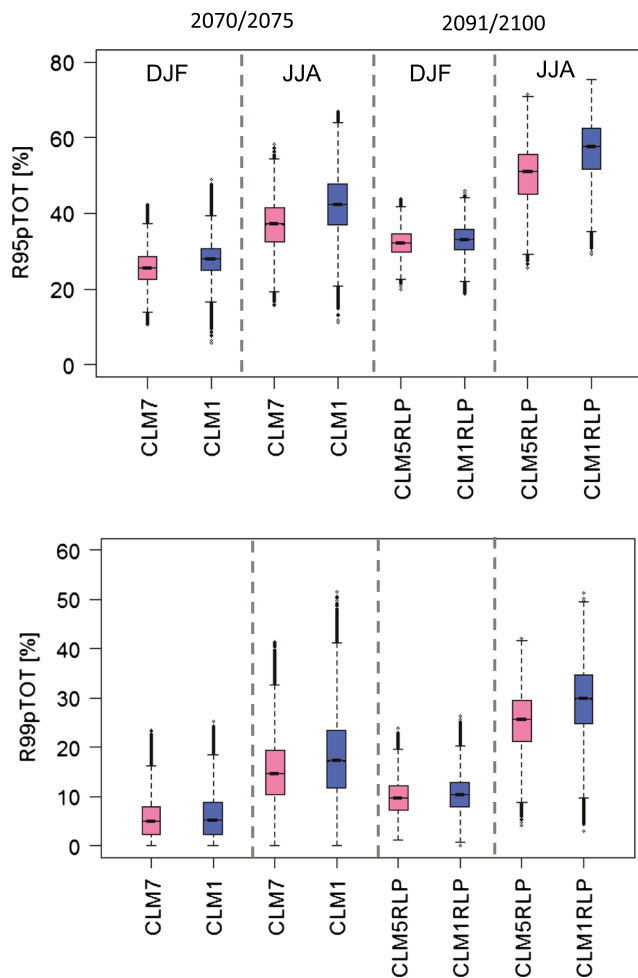


Fig. 12 Spatial distribution of seasonal future climate change of R95pTOT (upper panel) and R99pTOT (lower panel) summarized as box plots for simulation chains CLM7-CLM1 (left side) and CLM5RLP-CLM1RLP (right side). The base period for CLM7 and CLM1 is 1970–1975, and for CLM5RLP and CLM1RLP it is 1991–2000. Differences are significant at the 0.001 level. See Fig. 4 for abbreviations

period 1970–1975 for CLM7 and CLM1. The future period 2091–2100 with respect to the past period 1991–2000 is considered for CLM5RLP and CLM1RLP. The spatial distribution of seasonal changes and box plots of the ETCCDI indices are presented in Figs. 10, 11 and 12 for R99pTOT and R95pTOT, and those for TX90p are shown in Figs. 13 and 14, based on the IPCC scenario A1B.

3.7.1 Precipitation extremes

A comparison of results obtained with model chains CLM7-CLM1 and CLM5RLP-CLM1RLP for R99pTOT and R95pTOT presented in Figs. 10 and 11 indicates that the sign of the change signal remains the same for the simulations, but the magnitude of the signal is stronger

for CLM1 and CLM1RLP than for CLM7 and CLM5RLP. In particular, R99pTOT increases by 35% to 45%, and R95pTOT by 55% to 65%, in the highest resolution simulations in summer. These differences relative to the coarser simulations occur mainly over the lower land areas, where agriculture or grass is the dominant land use form (e.g. northwest or east of model domain, and valleys like Rhine valley), but also over mountainous areas (e.g. Elbe Sandstone Mountains). Because CLM7 produced higher mean rainfall amounts relative to CLM1, it is interesting that more pronounced increases in extreme precipitation occur for CLM1, especially in summer (see boxplots in Fig. 12) ($p < 0.001$ based on U test). Changes associated with resolution are weaker in winter for both extreme precipitation indices. These results also hold for CLM1RLP. In areas where extreme conditions are more frequent, extreme precipitation is predominantly caused by severe convection events. This phenomenon is not properly represented by RCMs at the coarse resolution investigated by Brisson et al. (2016), which led to observed underestimation. In the case of CLM7, there are still numerous processes that cannot be resolved explicitly and must be parameterized. These parameterizations, and in particular that of deep convection, have been identified as major sources of model errors and uncertainties (Arpagaus et al. 2009). The change signal of R95pTOT increases for all simulations compared with R99pTOT (see Fig. 11). The reason for the increase might be that the change in extremes is restricted to fewer extreme events in the upper tail of the distribution, but the amount of very extreme events, or their intensity, stays constant. There could also be fewer extreme events that are also stronger, but this differentiation is not shown with the index. In addition, R99pTOT and R95pTOT of CLM1 and CLM1RLP show more spatial variability compared with those of CLM7 and CLM5RLP, which is seen over the Rhine valley, the Black Forest, the Rothaar Mountains, and the Thuringian Highlands. Our findings are qualitatively in agreement with the increase in heavy precipitation found by Jacob et al. (2014). Because mountainous regions are a major landform over most areas of the world (Meybeck et al. 2001), our study may have a meaningful influence on climate change studies.

Based on these results, we conclude that the future change in the amount of extreme precipitation increases with higher resolution at convection-permitting scale, especially in summer.

3.7.2 Temperature extremes

In the case of seasonal extreme temperature changes (TX90p) (see Fig. 13), a fairly uniform pattern of changes with an east-west gradient in winter and a north-south gradient for RLP is projected under the assumption of scenario A1B. Changes are notably lower (-8%) for CLM1 and

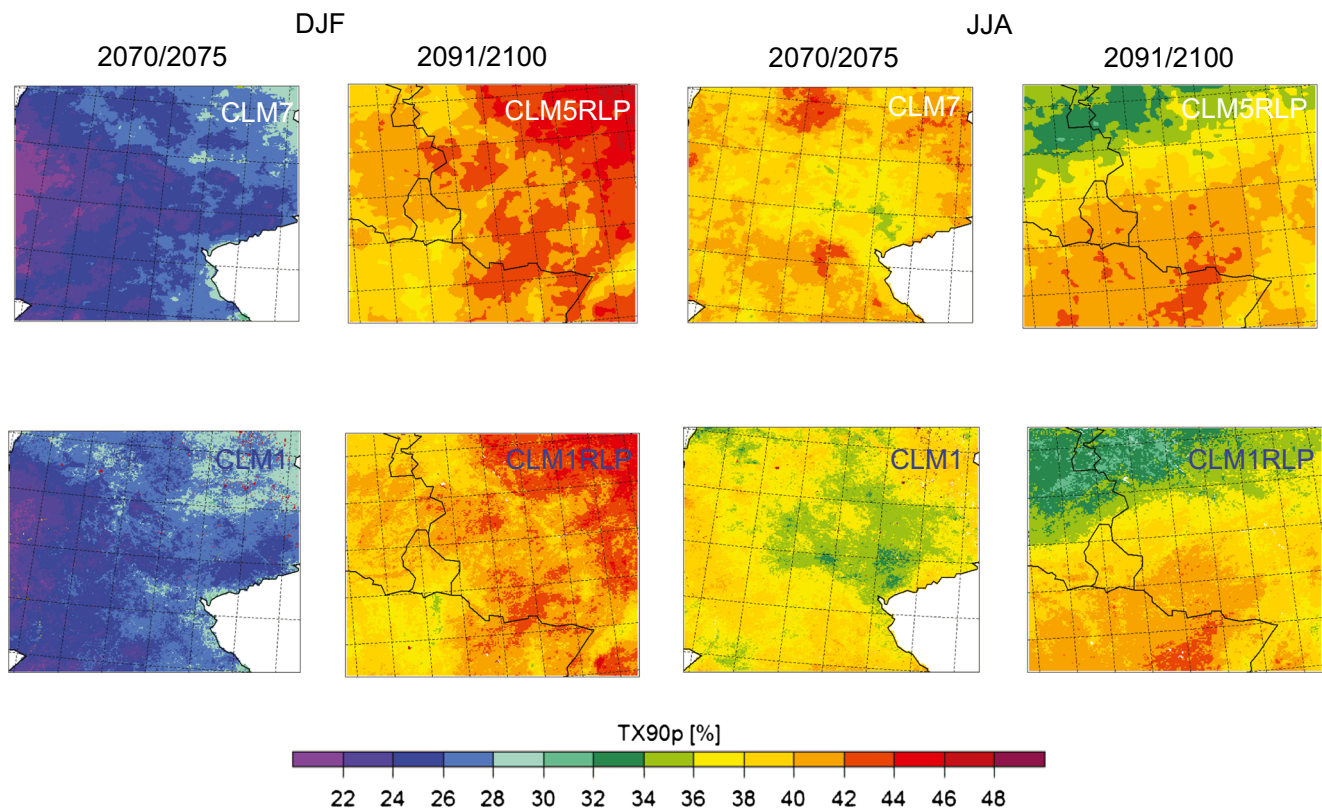


Fig. 13 Spatial distribution of seasonal future climate change of TX90p as a percentage change in a number of days of COSMO-CLM simulation chains CLM7-CLM1 (first and third column)

and CLM5RPLP-CLM1RPLP (second and fourth column). The base period for CLM7 and CLM1 is 1970–1975 and for CLM5RPLP and CLM1RPLP it is 1991–2000. See Fig. 4 for abbreviations

CLM1RPLP than for CLM7 and CLM5RPLP in summer (see boxplot in Fig. 14) ($p < 0.001$ based on U test). Extreme temperature decreases associated with higher resolution

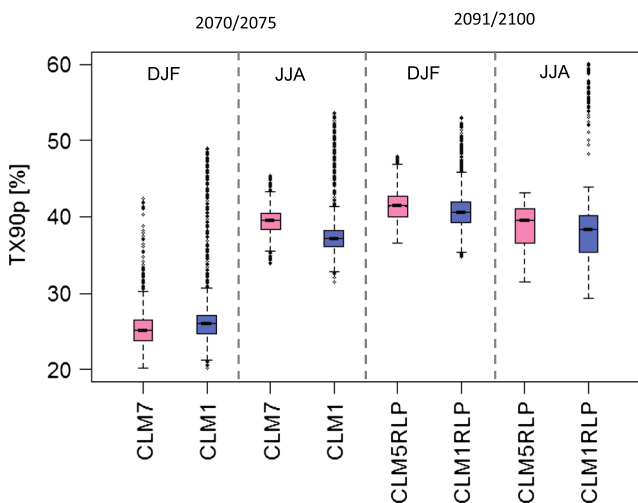


Fig. 14 Spatial distribution of future seasonal climate change of TX90p summarized as box plots for simulation chains CLM7-CLM1 (left side), and CLM5RPLP-CLM1RPLP (right side). The base period is 1970–1975 for CLM7 and CLM1, and 1991–2000 for CLM5RPLP and CLM1RPLP. Differences are significant at the 0.001 level. See Fig. 4 for abbreviations

are weaker for winter. Although changes are also higher for some grid boxes due to outliers in both seasons. There is a decrease of extreme events by 6% in CLM1RPLP relative to CLM5RPLP for the RLP region in winter ($p < 0.001$ based on U test). CLM1 shows a minor increase compared with CLM7 during this season. The multiple outliers in the distribution of TX90p for CLM1 may contribute to this result (see Fig. 14). Analysis of future climate change scenarios has shown that meteorological extreme temperature events are likely to increase in frequency (IPCC 2014). Here, we show that the amount of temperature extremes is lower for the higher-resolution simulations in summer, where temperature extremes are also expected to increase. We suggest that the analyzed changes are not caused by climate variability alone because they are strengthened by the analysis of two different areas and two different climate change periods, covering the period 2091–2100 versus 1991–2000, and the period 2070–2075 versus 1970–1975.

We conclude that for extreme maximum temperatures, the results indicate less future extreme events with higher resolution in summer. Although the differences between the resolutions considered in this work (7 and 1.3 km or 5 and 1.3 km) are small, we find that the differences in their changes in extreme temperatures is large.

4 Summary and conclusions

We have addressed the improvements and limitations resulting from increasing horizontal resolution in the regional climate model CCLM. Climate changes and changes of extreme values have been determined. The results for the analyzed mean fields reveal benefits of greater local detail with higher resolution. In some areas of orographically complex terrain, increasing resolution and convection-permitting simulations may improve results. Clear advancements are apparent for temperature and precipitation extremes, which are improved toward the observations with increasing resolution. Nevertheless, less clear spatial improvements could be found for extreme temperatures over mountain ridges. This analysis performed over the region of Germany can serve as an example for many other mid-latitude regions dominated by medium-sized mountains.

Overall, by downscaling to the highest spatial resolution (1.3 km), an inherent cold bias relative to the observations is introduced. The overestimation of precipitation is not reduced in either downscaling experiment (CLM7/CLM1, CLM5RLP/CLM1RLP) in winter. Precipitation of CLM1/CLM1RLP is close to the observations in summer.

For projections, our findings indicate less future warming in summer and more spatial variability of precipitation with fine-scale resolution regional climate modeling. Analysis of future climate change has shown that modeled precipitation extremes will be more severe, and temperature extremes will not exclusively increase with higher resolution. This information is important for regional impact and adaptation models to provide information for the water and energy sectors, agricultural activities, and planning and management development. Although the differences between the resolutions considered in this work (7 km/4.5 km and 1.3 km) are small, we find that the differences in the associated changes in extremes are large.

Although super-computing resources have enormously increased over the past decades, it is still expensive to perform multiple long-term high-resolution RCM simulations. Developing convection-permitting climate simulations is on the agendas of the regional climate modeling and impact communities, and is, therefore, highly relevant and of scientific interest. A more realistic representation of extreme indices is important for impact studies as these indices constitute valuable information in flood, drought and landslide studies. Developing convection-permitting simulations with combinations of parameterizations adapted accordingly is currently an ongoing effort of, for example, the CCLM community working group and EURO-CORDEX FPS on Convective Phenomena. Therefore, to benefit from high-resolution simulations, further studies are required, with

effective parameterizations and tunings for different topographic regions considered. This future work would support the discussion of climate projection uncertainty caused by model response. That is another step in that direction, and demonstrates that the effort to increase resolution in the RCM model may have valuable benefits in climate change information. Impact studies should be aware of the impact of model resolution on model processes and climate change.

Acknowledgements The authors thank the German Meteorological Service (DWD) for providing observational data, U. Blahak of the DWD for discussion of the results, and the COSMO-CLM community, the BMBF and the project leader PTJ for their support of the research activities in the framework of the BMBF-project BEST (BioEnergy STrengthening). The project was funded by the German Federal Ministry of Education and Research (BMBF), contract number 033L033A. Computational resources were made available by the German Climate Computing Center (DKRZ) through support from the BMBF.

Open Access This article is distributed under the terms of the Creative Commons Attribution 4.0 International License (<http://creativecommons.org/licenses/by/4.0/>), which permits unrestricted use, distribution, and reproduction in any medium, provided you give appropriate credit to the original author(s) and the source, provide a link to the Creative Commons license, and indicate if changes were made.

References

- Arpagaus M, Rotach MW, Ambrosetti P, Ament F, Appenzeller C, Bauer HS, Behrendt A, Bouttier F, Buzzi A, Corazza M, Davolio S, Denhard M, Dorninger M, Fontannaz L, Frick J, Fundel F, Germann U, Gorgas T, Grossi G, Hegg C, Hering A, Jaun S, Keil C, Liniger MA, Marsigli C, McTaggart-Cowan R, Montani A, Mylne K, Panziera L, Ranzani R, Richard E, Rossa A, Santos-Munoz D, Schär C, Seity Y, Staudinger M, Stoll M, Vogt S, Volkert H, Walser A, Wang Y, Werhahn J, Wulfmeyer V, Wunram C, Zappa M (2009) MAP D-PHASE: demonstrating forecast capabilities for flood events in the Alpine region. *MeteoSchweiz* 78:75
- Ban N, Schmidli J, Schär C (2014) Evaluation of the convection-resolving regional climate modeling approach in decade-long simulations. *J Geophys Res Atmos* 119:7889–7907. <https://doi.org/10.1002/2014JD021478>
- Ban N, Schmidli J, Schär C (2015) Heavy precipitation in a changing climate: does short-term summer precipitation increase faster? *Geophys Res Lett* 42:1165–1172. <https://doi.org/10.1002/2014GL062588>
- Berg P, Haerter JO, Thejll P, Piani C, Hagemann S, Christensen HJ (2009) Seasonal characteristics of the relationship between daily precipitation intensity and surface temperature. *J Geophys Res* 114:D18102. <https://doi.org/10.1029/2009JD01200>
- Berg P, Wagner S, Kunstmann H, Schädler G (2013) High resolution regional climate model simulations for Germany: part I - validation. *Clim Dyn* 40(1–2):401–414. <https://doi.org/10.1007/s00382-012-1508-8>
- Brisson E, Weverberg KV, Demuzere M, Devis A, Saeed S, Stengel M, van Lipzig NPM (2016) How well can a convection-permitting climate model reproduce decadal statistics of precipitation, temperature and cloud characteristics? *Clim Dyn* 47(9–10):3043–3061. <https://doi.org/10.1007/s00382-016-3012-z>

- Bucchignani E, Montesarchio M, Zollo AL, Mercogliano P (2016) High-resolution climate simulations with COSMO-CLM over Italy: performance evaluation and climate projections for the 21st century. *Int J Climatol* 36:735–756. <https://doi.org/10.1002/joc.4379>
- Champeaux JL, Masson V, Chauvin F (2005) Ecoclimap: a global database of land surface parameters at 1 km resolution. *Meteorol Appl* 12:29–32. <https://doi.org/10.1017/S1350482705001519>
- Chan SC, Kendon EJ, Fowler HJ, Blenkinsop S, Roberts NM (2014a) Projected increases in summer and winter UK sub-daily precipitation extremes from high-resolution regional climate models. *Environ Res Lett* 9(084019):9. <https://doi.org/10.1088/1748-9326/9/8/084019>
- Chan SC, Kendon EJ, Fowler HJ, Blenkinsop S, Roberts NM, Ferro CAT (2014b) The value of high-resolution met office regional climate models in the simulation of multihourly precipitation extremes. *J Clim* 27(16):6155–6174. <https://doi.org/10.1175/JCLI-D-13-00723.1>
- Christensen JH, Christensen OB (2007) A summary of the PRUDENCE model projections: changes in European climate by the end of this century. *Climate Change* 81:7–30. <https://doi.org/10.1007/s10584-006-9210-7>
- Christensen JH, Hewitson B, Busiuc A, Chen A, Gao X, Held I, Jones R, Kolli RK, Kwon WT, Laprise R, Rueda VM, Mearns L, Menendez CG, Räisänen J, Rinke A, Sarr A, Whetton P (2007) Regional climate projections. In: *Climate change 2007: the physical science basis. Contribution of working group I to the fourth assessment report of the intergovernmental panel on climate change*. Cambridge University Press, Cambridge, United Kingdom
- Dee DP, Uppala SM, Simmons AJ, Berrisford P, Poli P, Kobayashi S, Andrae U, Balmaseda MA, Balsamo G, Bauer P, Bechtold P, Beljaars ACM, van de Berg L, Bidlot J, Bormann N, Delsol C, Dragani R, Fuentes M, Geer AJ, Haimberger L, Healy SB, Hersbach H, Hólm EV, Isaksen L, Kållberg P, Köhler M, Matricardi M, McNally AP, Monge-Sanz BM, Morcrette JJ, Park BK, Peubey C, de Rosnay P, Tavolato C, Thépaut JN, Vitart F (2011) The ERA-interim reanalysis: configuration and performance of the data assimilation system. *Q J R Meteorol Soc* 137(656):553–597. <https://doi.org/10.1002/qj.828>
- Doms G, Baldauf M (2015) A description of the nonhydrostatic regional COSMO-model Part I: dynamics and numerics consortium for small-scale modelling. Technical report Deutscher Wetterdienst, Offenbach, Germany
- Evans JP, McCabe MF (2013) Effect of model resolution on a regional climate model simulation over Southeast Australia. *Clim Res* 56:131–145. <https://doi.org/10.3354/cr01151>
- Fosser G, Khodayar S, Berg P (2015) Benefit of convection permitting climate model simulations in the representation of convective precipitation. *Clim Dyn* 44(1–2):45–60. <https://doi.org/10.1007/s00382-014-2242-1>
- Fosser G, Khodayar S, Berg P (2016) Climate change in the next 30 years: what can a convection-permitting model tell us that we did not already know? *Clim Dyn* 48(5–6):1987–2003. <https://doi.org/10.1007/s00382-016-3186-4>
- Frick C, Steiner H, Mazurkiewicz A, Riediger U, Rauthe M, Reich T, Gratzki A (2014) Central european high-resolution gridded daily data sets (HYRAS): mean temperature and relative humidity. *Meteorol Z* 23(1):15–32. <https://doi.org/10.1127/0941-2948/2014/0560>
- Froidevaux P, Schlemmer L, Schmidli J, Langhans W, Schär C (2014) Influence of the background wind on the local soil moisture-precipitation feedback. *J Atmos Sci* 71:782–799. <https://doi.org/10.1175/JAS-D-13-0180.1>
- Giorgi F, Jones C, Asrar GR (2009) Addressing climate information needs at the regional level: the CORDEX framework. *World Meteorological Organization (WMO) Bulletin* 58(3):175
- Giorgi F, Torma C, Coppola E, Ban N, Schär C, Somot S (2016) Enhanced summer convective rainfall at Alpine high elevations in response to climate warming. *Nat Geosci* 9:584–589. <https://doi.org/10.1038/ngeo2761>
- Gutjahr O, Schefczyk L, Reiter P, Heinemann G (2016) Impact of the horizontal resolution on the simulation of extremes. *Meteorol Z* 25(5):543–562. <https://doi.org/10.1007/s00704-013-0834-z>
- Haslinger K, Anders I, Hofstätter M (2013) Regional climate modelling over complex terrain: an evaluation study of COSMO-CLM hindcast model runs for the Greater Alpine Region. *Clim Dyn* 40:511–529. <https://doi.org/10.1007/s00382-012-1452-7>
- Haylock MR, Hofstra N, Tank AMGK, Klok EJ, Jones PD, New M (2008) A European daily high-resolution gridded data set of surface temperature and precipitation for 1950–2006. *J Geophys Res* 113:D20119. <https://doi.org/10.1029/2008JD010201>
- Heise E, Ritter B, Schrodin R (2006) Operational implementation of the multilayer soil model. Technical report, COSMO Tech. Rep., No. 9
- Herrera S, Fita L, Fernández J, Gutiérrez JM (2010) Evaluation of the mean and extreme precipitation regimes from the ENSEMBLES regional climate multimodel simulations over Spain. *J Geophys Res* 15:D21117. <https://doi.org/10.1029/2010JD013936>
- Hewitt CD (2004) Ensembles-based predictions of climate changes and their impacts. *Eos Trans AGU* 85(52):566. <https://doi.org/10.1029/2004EO520005>
- Hohenegger C, Brockhaus P, Schär C (2008) Towards climate simulations at cloud-resolving scales. *Meteorol Z* 17(4):383–394. <https://doi.org/10.1127/0941-2948/2008/0303>
- Hohenegger C, Brockhaus P, Bretherton S, Schär C (2009) The soil moisture-precipitation feedback in simulations with explicit and parameterized convection. *J Clim* 22(19):5003–5020. <https://doi.org/10.1175/2009JCLI2604.1>
- Hollweg HJ, Böhm U, Fast I, Hennemuth B, Keuler K, Keup-Thiel E, Lautenschlager M, Legutke S, Radtke K, Rockel B, Schubert M, Will A, Woldt M, Wundram C (2008) Ensemble simulations over Europe with the regional climate model CLM forced with IPCC AR4 global scenarios. Technical Report 3, Model and Data Group at the Max Planck Institute for Meteorology, Hamburg
- IPCC (2007) Emission scenarios. Cambridge University Press, Cambridge, United Kingdom
- IPCC (2014) Climate change 2014: Synthesis report. Contribution of working groups I, II and III to the fifth assessment report of the intergovernmental panel on climate change IPCC, Geneva, Switzerland
- Jacob D, Barring L, Christensen OB, Christensen JH, de Castro M, Dequé M, Giorgi F, Hagemann S, Hirschi M, Jones R, Kjellström E, Lenderink G, Rockel B, Sanchez E, Schär C, Seneviratne SI, Somot S, van Ulden A, van den Hurk B. (2007) An inter-comparison of regional climate models for Europe: model performance and present-day climate. *Clim Chang* 81:31–52. <https://doi.org/10.1007/s10584-006-9213-4>
- Jacob D, Bülow K, Kotova L, Moseley C, Petersen J, Recchid D (2012) Regionale klimaprojektionen für europa und deutschland: ensemble-simulationen für die klimafolgenforschung. CSC report 6, Climate Service Center
- Jacob D, Petersen J, Eggert B, Alias A, Christensen OB, Bouwer LM, Braun A, Colette A, Déqué M, Georgievski G, Georgopoulou E, Gobiet A, Menut L, Nikulin G, Haensler A, Hempelmann N, CJ C, Keuler K, Kovats S, Kröner N, Kotlarski S, Kriegsmann A, Martin E, vanMeijgaard E, Moseley C, Pfeifer S, Preuschmann S, Radermacher C, Radtke K, Rechid D, Rounsevell M, Samuelsson P, Somot S, Soussana JF, Teichmann C, Valentini R, Vautard R, Weber B, Yiou P (2014) EURO-CORDEX: new high-resolution climate change projections for European impact research. *Reg Environ Chang* 14:563–578. <https://doi.org/10.1007/s10113-013-0499-2>

- Kendon EJ, Roberts NM, Fowler HJ, Roberts MJ, Chan SC, Senior CA (2014) Heavier summer downpours with climate change revealed by weather forecast resolution model. *Nat Clim Chang* 4:570–576. <https://doi.org/10.1038/nclimate2258>
- Knote C, Heinemann G, Rockel B (2010) Changes in weather extremes: assessment of return values using high resolution climate simulations at convection-resolving scale. *Meteorol Z* 19(1):11–23. <https://doi.org/10.1127/0941-2948/2010/0424>
- Kotlarski S, Block A, Böhm U, Jacob D, Keuler K, Knoche R, Rechid D, Walter A (2005) Regional climate model simulations as input for hydrological applications: evaluation of uncertainties. *Advancements of Geosciences* 5:119–125. <https://doi.org/10.5194/adgeo-5-119-2005>
- Kotlarski S, Keuler K, Christensen OB, Colette A, Déqué M, Gobiet A, Georgen K, Jacob D, Lüthi D, van Meijgaard E, Nikulin G, Schär C, Teichmann C, Vautard R, Warrach-Sagi K, Wulfmeyer V (2014) Regional climate modeling on European scales: a joint standard evaluation of the EURO-CORDEX RCM ensemble. *Geosci Model Dev* 7:1297–1333. <https://doi.org/10.5194/gmd-7-1297-2014>
- Lind P, Lindstedt D, Kjellström E, Jones C (2016) Spatial and temporal characteristics of summer precipitation over Central Europe in a suite of high-resolution climate models. *J Clim* 29:3501–3518. <https://doi.org/10.1175/JCLI-D-15-0463.1>
- Luca AD, de Elia R, Laprise R (2012) Potential for added value in precipitation simulated by high-resolution nested regional climate models and observations. *Clim Dyn* 38:1229–1247
- Macadam I, Pitman A, Whetton P, Abramowitz G (2010) Ranking climate models by performance using actual values and anomalies: implications for climate change impact assessments. *Geophys Res Lett* 37:L16704. <https://doi.org/10.1029/2010GL043877>
- Maraun D, Wetterhall F, Ireson AM, Chandler RE, Kendon EJ, Widmann W, Brienen S, Rust HW, Sauter T, Themeßl M, Venema VKC, Chun KP, Goodess CM, Jones RG, Onof C, Vrac M, Thiele-Eich I (2010) Precipitation downscaling under climate change: recent developments to bridge the gap between dynamical models and the end user. *Rev Geophys* 48:RG3003. <https://doi.org/10.1029/2009RG000314>
- Meybeck M, Green P, Vörösmarty C (2001) A new typology for mountain and other relief classes. *Mt Res Dev* 21(1):34–45. [https://doi.org/10.1659/0276-4741\(2001\)021<0034::Anewtypologyfor>2.0.co;2](https://doi.org/10.1659/0276-4741(2001)021<0034::Anewtypologyfor>2.0.co;2)
- Montesarchio M, Zollo AL, Bucchignani E, Mercogliano P, Castellari S (2014) Performance evaluation of high-resolution regional climate simulations in the alpine space and analysis of extreme events. *J Geophys Res Atmos* 119:3222–3237. <https://doi.org/10.1002/2013JD021105>
- Prein AF, Gobiet A, Suklitsch M, Truhetz H, Keuler NKA, Georgievski G (2013) Added value of convection permitting seasonal simulations. *Clim Dyn* 41:2655–2677. <https://doi.org/10.1007/s00382-013-1744-6>
- Prein AF, Langhans W, Fossier G, Ferrone A, Ban N, Georgen K, Keller M, Tölle M, Gutjahr O, Feser F, Brisson E, Kollet S, Schmidli J, Lipzig NV, Leung R (2015) A review on regional convection-permitting climate modeling: demonstrations, prospects, and challenges. *Rev Geophys*:53. <https://doi.org/10.1029/2014RG000475>
- Raschendorfer M (2001) The new turbulence parameterization of LM. Technical report, COSMO newsletter1, Deutscher Wetterdienst, Offenbach, Germany
- Rauscher S, Coppola E, Piani C, Giorgi F (2010) Resolution effects on regional climate model simulations of seasonal precipitation over Europe. *Clim Dyn* 35(4):685–711. <https://doi.org/10.1007/s00382-009-0607-7>
- Rauthe M, Steiner H, Riediger U, Mazurkiewicz A, Gratzki A (2013) A Central European precipitation climatology - Part I: generation and validation of a high-resolution gridded daily data set (HYRAS). *Meteorol Z* 22(3):235–256. [https://doi.org/10.1175/1520-0493\(1992\)120](https://doi.org/10.1175/1520-0493(1992)120)
- Ritter B, Geleyn JF (1992) A comprehensive radiation scheme for numerical weather prediction models with potential applications in climate simulations. *Mon Weather Rev* 120:303–325
- Rockel B, Will A, Hense A (2008) The regional climate model COSMO-CLM (CCLM). *Meteorol Z* 17(4):347–348. <https://doi.org/10.1127/0941-2948/2008/0309>
- Roeckner E, Brokopf R, Esch M, Giorgetta M, Hagemann S, Kornbluh L (2006) Sensitivity of simulated climate to horizontal and vertical resolution in the ECHAM5 atmosphere model. *J Clim* 19:3771–3791. <https://doi.org/10.1175/JCLI3824.1>
- Schättler U, Doms G, Schraff C (2009) A description of the nonhydrostatic regional COSMO-model Part VII: user's guide. Consortium for small-scale modelling. *COSMO Model* 4:11
- Schefczyk L, Heinemann G (2017) Climate change impact on thunderstorms: analysis of thunderstorm indices using high-resolution regional climate simulations. *Meteorol Z*. <https://doi.org/10.1127/metz/2017/0749>
- Smiatek G, Rockel B, Schättler U (2008) Time invariant data preprocessor for the climate version of the COSMO model (COSMO-CLM). *Meteorol Z* 17(4):395–405. <https://doi.org/10.1127/0941-2948/2008/0302>
- Stappeler J, Doms G, Schättler U, Bitzer HW, Gassmann A, Damrath U, Gregoric G (2003) Meso-gamma scale forecasts using the nonhydrostatic model LM. *Meteorol Atmos Phys* 82(1–4):75–96. <https://doi.org/10.1007/s00703-001-0592-9>
- Tank AMGK, Zwiers FW, Zhang X (2009) Guidelines on analysis of extremes in a changing climate in support of informed decisions for adaptation. Technical Report WCDMP-no. 72, WMO
- Tiedtke M (1989) A comprehensive mass flux scheme for cumulus parameterization in largescale models. *Mon Weather Rev* 117:1779–1800. [https://doi.org/10.1175/1520-0493\(1989\)117](https://doi.org/10.1175/1520-0493(1989)117)
- Tölle MH, Gutjahr O, Thiele JC, Busch G (2014) Increasing bioenergy production on arable land - does the regional and local climate respond? Germany as a case study. *J Geophys Res* 119:2711–2724. <https://doi.org/10.1002/2013JD020877>
- Trenberth KE, Dai A, Rasmussen RM, Parsons DB (2003) The changing character of precipitation. *Bull Am Meteorol Soc* 84:1205–1217. <https://doi.org/10.1175/BAMS-84-9-1205>
- Tselioudis G, Douvis C, Zerefos C (2012) Does dynamical downscaling introduce novel information in climate model simulations of precipitation change over a complex topography region? *Int J Climatol* 32:1572–1578. <https://doi.org/10.1002/joc.2360>
- USGS (1996) USGS, GTOPO30 documentation. Technical report, U.S. Geological Survey
- van der Linden P, Mitchell JFB (2009) ENSEMBLES: climate change and its impacts: summary of research and results from the ENSEMBLES project. Technical report, Met Office Hadley Centre, Fitz Roy Road, Exeter EX1 3PB, UK, 160
- Vautard R, Gobiet A, Jacob D, Belda M, Colette A, Déqué M, Fernández J, García-Díez M, Goergen K, Güttler I, Halenka T, Katragkou TKE, Keuler K, Kotlarski S, Mayer S, van Meijgaard E, Nikulin G, Patarcic M, Scinocca J, Sobolowski S, Suklitsch M, Teichmann C, Warrach-Sagi K, Wulfmeyer V, Yiou P (2013) The simulation of European heat waves from an ensemble of regional climate models within the EURO-CORDEX project. *Clim Dyn* 41:2555–2575. <https://doi.org/10.1007/s00382-013-1714-z>
- von Storch H, Zwiers FW (1999) Statistical analysis in climate research. Cambridge University Press, Cambridge, United Kingdom
- Walsh K, McGregor J (1997) An assessment of simulations of climate variability over Australia with a limited area model. *Int J Climatol* 17:201–223. [https://doi.org/10.1002/\(SICI\)1097-0088\(199702\)17](https://doi.org/10.1002/(SICI)1097-0088(199702)17)
- Warrach-Sagi K, Schwitalla T, Wulfmeyer V, Bauer HS (2013) Evaluation of a climate simulation in Europe based on the WRF-NOAH

- model system: precipitation in Germany. *Clim Dyn* 41(3–4):755–774. <https://doi.org/10.1007/s00382-013-1727-7>
- Wicker LJ, Skamarock WC (2002) Time-splitting methods for elastic models using forward time schemes. *Mon Weather Rev* 130:2088–2097. [https://doi.org/10.1175/1520-0493\(2002\)130](https://doi.org/10.1175/1520-0493(2002)130)
- Zollo AL, Rillo V, Bucchignani E, Montesarchio M, Mercogliano P (2015) Extreme temperature and precipitation events over Italy: assessment of high-resolution simulations with COSMO-CLM and future scenarios. *Int J Climatol* 36(2):987–1004. <https://doi.org/10.1002/joc.4401>
- Zubler EM, Fischer AM, Fröb F, Liniger MA (2015) Climate change signals of CMIP5 general circulation models over the Alps - impact of model selection. *Int J Climatol* 36(8):3088–3104. <https://doi.org/10.1002/joc.4538>